Vertical distribution of phytoplankton communities in open ocean: An assessment based on surface chlorophyll

Julia Uitz, Hervé Claustre, Andre Morel, Stanford B. Hooker

Vertical distribution of phytoplankton communities in open ocean: An assessment based on surface chlorophyll

Julia Uitz,[1] Hervé Claustre,[1] André Morel,[1] and Stanford B. Hooker[2]

Received 5 August 2005; revised 22 December 2005; accepted 31 March 2006; published 2 August 2006.

[1] The present study examines the potential of using the near-surface chlorophyll *a* concentration ($[\mathrm{Chl}a]_{\mathrm{surf}}$), as it can be derived from ocean color observation, to infer the column-integrated phytoplankton biomass, its vertical distribution, and ultimately the community composition. Within this context, a large High-Performance Liquid Chromatography (HPLC) pigment database was analyzed. It includes 2419 vertical pigment profiles, sampled in case 1 waters with various trophic states (0.03–6 mg Chl*a* m^{-3}). The relationships between $[\mathrm{Chl}a]_{\mathrm{surf}}$ and the chlorophyll *a* vertical distribution, as previously derived by Morel and Berthon (1989), are fully confirmed. This agreement makes it possible to go further and to examine if similar relationships between $[\mathrm{Chl}a]_{\mathrm{surf}}$ and the phytoplankton assemblage composition along the vertical can be derived. Thanks to the detailed pigment composition, and use of specific pigment biomarkers, the contribution to the local chlorophyll *a* concentration of three phytoplankton groups can be assessed. With some cautions, these groups coincide with three size classes, i.e., microplankton, nanoplankton and picoplankton. Corroborating previous regional findings (e.g., large species dominate in eutrophic environments, whereas tiny phytoplankton prevail in oligotrophic zones), the present results lead to an empirical parameterization applicable to most oceanic waters. The predictive skill of this parameterization is satisfactorily tested on a separate data set. With such a tool, the vertical chlorophyll *a* profiles of each group can be inferred solely from the knowledge of $[\mathrm{Chl}a]_{\mathrm{surf}}$. By combining this tool with satellite ocean color data, it becomes possible to quantify on a global scale the phytoplankton biomass associated with each of the three algal assemblages.

Citation: Uitz, J., H. Claustre, A. Morel, and S. B. Hooker (2006), Vertical distribution of phytoplankton communities in open ocean: An assessment based on surface chlorophyll, *J. Geophys. Res.*, *111*, C08005, doi:10.1029/2005JC003207.

1. Introduction

[2] A quasi-permanent monitoring of the algal content of the sunlit world ocean is only achievable by satellite observation of "ocean color." The sea spectral reflectance, as detected by a remote sensor, can provide an estimate of the chlorophyll *a* concentration, which is commonly used as an index of the algal biomass. This estimate, however, is restricted to the upper layer of the water column only [*Gordon and McCluney*, 1975]. Within the context of ecological studies dealing with the vertical distribution of algal species, as well as for biogeochemical applications involving primary production, such satellite information about the near-surface layer is insufficient. Indeed, the assessment of the algal biomass must be extended downward in order to encompass the entire depth range where algae can live and grow. For instance, the transformation of "chlorophyll maps" as obtained from spaceborne sensors into "primary production maps" [*Campbell et al.*, 2002], through the use of light-photosynthesis models, requires at least that the column-integrated algal biomass is known, and better, that the biomass vertical distribution within the decreasingly illuminated layers can be in some way described. The terms "known" or "described" actually mean "assumed" or "predicted" for each pixel of a satellite image with a sufficient degree of confidence. The creation of such a predictive capability was the main motivation of the first study carried out by *Morel and Berthon* [1989, hereinafter referred to as MB89].

[3] The heuristic hypothesis in MB89 was that the near-surface chlorophyll concentration is in some manner related to the column-integrated chlorophyll content, and even to the shape of the phytoplankton vertical distribution. The validity of this initial working hypothesis was amply demonstrated through the examination, and then the statistical analysis, of about 4000 vertical profiles of chlorophyll *a* concentration, determined in oceanic case 1 waters only [*Gordon and Morel*, 1983], and with near-surface concentrations varying over more than two orders of magnitude. The main conclusions of the MB89 study were as follows: (1) The integrated chlorophyll *a* biomass over the euphotic

[1] Laboratoire d'Océanographie de Villefranche, CNRS UMR 7093, and Université Pierre et Marie Curie, Villefranche-sur-Mer, France.
[2] Laboratory for Hydrospheric Processes, NASA/Goddard Space Flight Center, Greenbelt, Maryland, USA.

0148-0227/06/2005JC003207

Table 1. Symbols Used in the Present Study and Their Significance

Symbol	Significance
Chl*a*	total chlorophyll *a* (chlorophyll *a* + divinyl chlorophyll *a* + chlorophyllid *a* + chlorophyll *a* allomers and epimers)
[Chl*a*]	Chl*a* concentration, mg m^{-3}
[P]	concentration of pigment P, mg m^{-3}
PAR	photosynthetically available radiation, W m^{-2}
Z_{pd}	penetration depth, m
$[Chla]_{surf}$	average total chlorophyll *a* within the surface layer $0-Z_{pd}$, mg m^{-3}
z	geometrical depth, m
Z_{eu}	depth of the euphotic layer, defined as the depth where the PAR is reduced to 1% of its surface value, m
ζ	depth normalized with respect to Z_{eu}: $\zeta = z/Z_{eu}$, dimensionless
$\langle Chla \rangle_{Zeu}$	Chl*a* column-integrated content, within the euphotic layer, mg m^{-2}
$\langle Chla \rangle_{1.5\ Zeu}$	Chl*a* column-integrated content, within the $0-1.5\ Z_{eu}$ layer, mg m^{-2}
$\overline{Chla}_{Zeu}$	average column-integrated content of total chlorophyll *a* within the euphotic layer, mg m^{-3}
$P(\zeta)$	concentration of pigment P, at (the dimensionless depth) ζ, mg m^{-3}
$p(\zeta)$	concentration of pigment P normalized with respect to $\overline{Chla}_{Zeu}$, $p(\zeta) = P(\zeta)/\overline{Chla}_{Zeu}$, dimensionless
micro-Chl*a*	total chlorophyll *a* associated to microplankton
nano-Chl*a*	total chlorophyll *a* associated to nanoplankton
pico-Chl*a*	total chlorophyll *a* associated to picoplankton
f_{micro}	fraction of Chl*a* associated to microplankton
f_{nano}	fraction of Chl*a* associated to nanoplankton
f_{pico}	fraction of Chl*a* associated to picoplankton
Z_m	depth of the mixed layer, m
$[P]_{max}$	maximum concentration on a considered P vertical profile, mg m^{-3}
Z_{max}	depth of $[P]_{max}$, m

layer (mg m^{-2}) and the near-surface chlorophyll *a* concentration (mg m^{-3}) are highly correlated, albeit in a nonlinear fashion. (2) The vertical chlorophyll *a* profiles in stratified waters can be orderly sorted into several ''trophic categories,'' on the basis of the near-surface chlorophyll *a* concentration, and (3) each of these categories exhibits, in a statistical sense, a typical chlorophyll *a* vertical profile, which generally includes a somewhat pronounced, and more or less deep, chlorophyll *a* maximum; (4) for such vertically stratified waters, a parameterization was proposed which allowed the vertical structure of the chlorophyll *a* profiles to be predicted in a continuous manner from the near-surface chlorophyll *a* value alone; and finally, (5) the separate statistical analysis of vertically well mixed waters (essentially in high latitudes and in winter) showed that the vertical chlorophyll *a* profiles are essentially uniform (as intuitively expected).

[4] The present study is chiefly motivated by the considerable improvement brought by the introduction, and systematic use, of High-Performance Liquid Chromatography (HPLC) for determining the concentration of marine pigments. Indeed, in the frame of national and international programs such as Joint Global Ocean Flux Study (JGOFS), HPLC pigment analyzes have been systematically carried out during at least the last decade; once merged, these data constitute an incomparable set for global ocean studies like the present one. Before proceeding further, the logical first goal of the present study is, therefore, to check the validity of the initial working hypothesis of MB89, and to confirm or modify the global description they proposed, by considering another data set, which is based on another analytical method.

[5] Beyond this first objective, it is now possible to delve deeper into the analysis. Indeed, it becomes increasingly obvious that the use of only chlorophyll *a* as a proxy for the algal biomass remains insufficient, as far as oceanic biogeochemical cycles are to be studied and ultimately modeled. In effect, the ''quality'' of the phytoplankton populations (in particular their taxonomic composition) impacts on, or reciprocally, is a signature of, specific biogeochemical processes. For example, tiny phytoplankton are preferentially associated with the presence of regenerated forms of the nutrients they are able to utilize, whereas large phytoplankters (diatoms), which are more involved in so-called new production, develop preferentially when fresh nutrients become available [*Eppley and Peterson*, 1979; *Malone*, 1980; *Goldman*, 1993]. A relationship between the (instantaneous) trophic status of a water body, as locally depicted by the near-surface chlorophyll *a* content, and the local taxonomic composition of the algal assemblage can reasonably be expected [*Claustre*, 1994], and is worth pursuing.

[6] The HPLC method allows the assessment of the so-called ''total'' chlorophyll *a* concentration; this quantity will be simply noted [Chl*a*] (see Table 1 for a list of symbols). More importantly, the HPLC method also allows a suite of accessory pigments (carotenoids and chlorophylls) to be determined. Many of these pigments are specific of individual phytoplanktonic taxa or groups [*Jeffrey and Vesk*, 1997]. They can thus be used as biomarkers of various phytoplankton groupings [e.g., *Gieskes et al.*, 1988; *Prézelin et al.*, 2000], and with some cautions assigned to different size classes, such as microphytoplankton, nanophytoplankton and picophytoplankton [*Vidussi et al.*, 2001]. Consequently, the column-integrated biomasses of each of the algal classes, as well as their vertical profiles, can be determined from the details of the vertical distribution of the pigment composition. As a result, the respective contribution of each class to the total standing algal stock can be assessed. The second objective of the present study is, therefore, to examine, on the basis of the analysis of HPLC data, whether some generic properties regarding the composition and vertical distribution of the various phytoplankton assemblages may be predicted from the near-surface

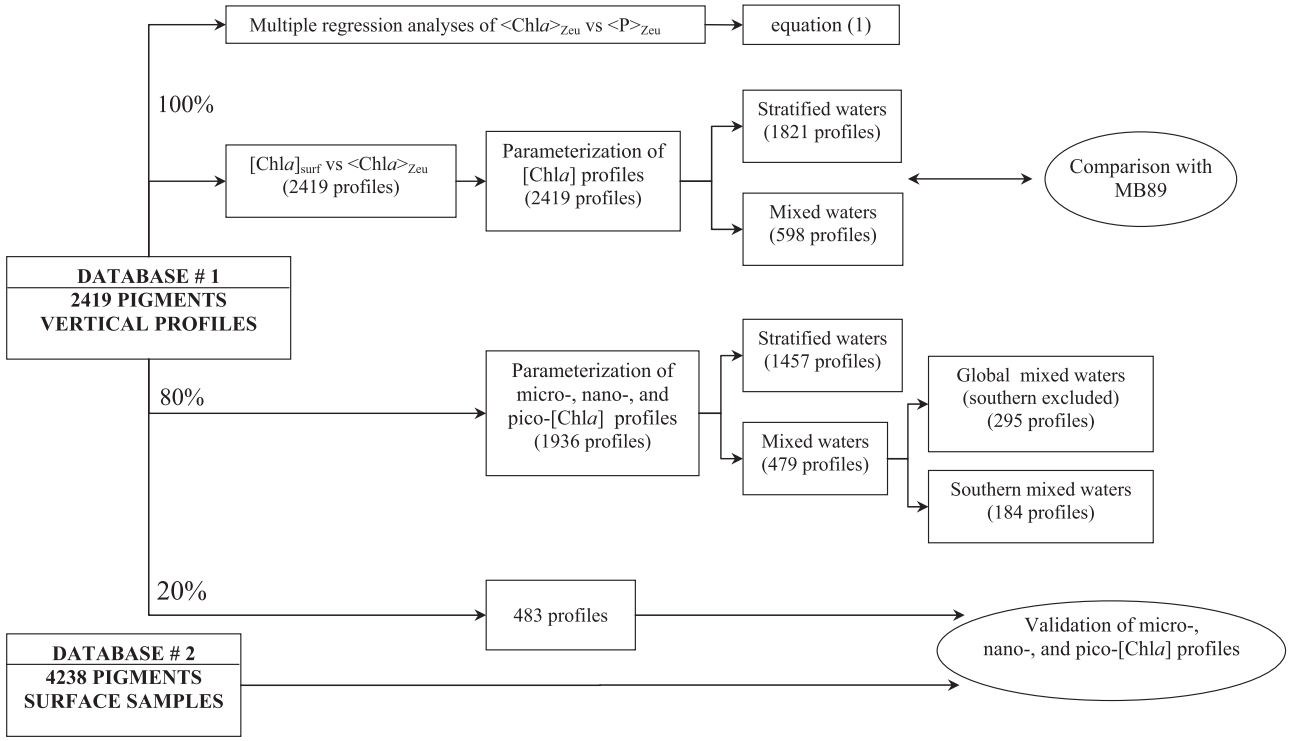

Figure 1. A flowchart showing the partition and the use of the two data sets (after quality control) for subsequent analyses.

total chlorophyll *a* concentration (hereinafter denoted $[\mathrm{Chl}a]_{\mathrm{surf}}$).

2. Phytoplankton Pigment Database

[7] To achieve the aforementioned objectives, a large HPLC pigment database, resulting from numerous field campaigns (about 120 cruises which mainly occurred during the last decade; Tables S1 and S2 in auxiliary material[1]) was analyzed. It encompasses stations sampled in case 1 waters in various hydrological and trophic conditions (ranging from oligotrophic to eutrophic situations). A statistical analysis of this database is carried out to extract, and then parameterize, the relationships between $[\mathrm{Chl}a]_{\mathrm{surf}}$ and (1) the chlorophyll *a* vertical content and distribution (as previously done in MB89), (2) the phytoplanktonic community composition in the upper layer, and (3) the vertical layering of these communities.

[8] Actually, two (independent) pigment databases are used in the present study. The first one includes about 2950 vertical profiles, whereas the second one includes about 4870 samples restricted to near-surface waters only. The former is used to perform statistical analyses of the shape of, and algal composition within, the vertical profiles. The latter is used exclusively for validating the statistical relationships between $[\mathrm{Chl}a]_{\mathrm{surf}}$ and the phytoplanktonic composition within the surface layer. The analysis methodology of using these databases is schematically presented in Figure 1.

[9] The geographic distribution of the stations included in database 1 is uneven (Figure 2a). The Mediterranean Sea and the Atlantic and Pacific Oceans are well represented (especially the subtropical gyres of the northern basins), but the South Pacific Subtropical Gyre and the Indian Ocean are less sampled. The stations in the Southern Ocean are mostly located in the Ross Sea, and there are no data from the Arctic Ocean. The statistical distribution of the stations of database 1 with respect to their near-surface chlorophyll concentration is displayed on Figures 2b and 2c (for stratified and mixed waters, respectively (see later on)). The frequency distribution for stratified waters (Figure 2b) is close to that observed for the SeaBAM data set which deals only with surface chlorophyll [*O'Reilly et al.*, 1998]. With a mean (and median) value of 0.184 mg m^{-3}, the shape of the frequency distribution is similar to that derived for the whole ocean from ocean color imagery (mean value 0.21–0.26 mg m^{-3} [*Antoine et al.*, 2005]). Therefore the data set can be considered as representative of the global ocean, even if very low and very high chlorophyll values are not well represented here (by lack of data). For mixed water, the range of chlorophyll values is wider (up to 10 mg m^{-3}), with a considerably higher mean value (0.78 mg m^{-3}). The database 2 includes primarily data from the Atlantic Ocean; they were collected either during cruises not contributing to the first database, or, if acquired during the same cruises, at locations differing from those where the vertical profiles were collected (e.g., surface samples taken along transects between stations).

2.1. Overall Quality Assurance

[10] Because the field samples were collected by several teams, and analyzed in different laboratories using a variety of HPLC instruments and protocols, a quality assurance process is needed to ensure that the data sets can be combined coherently.

[1] Auxiliary materials are available in the HTML. doi: 10.1029/2005JC003207.

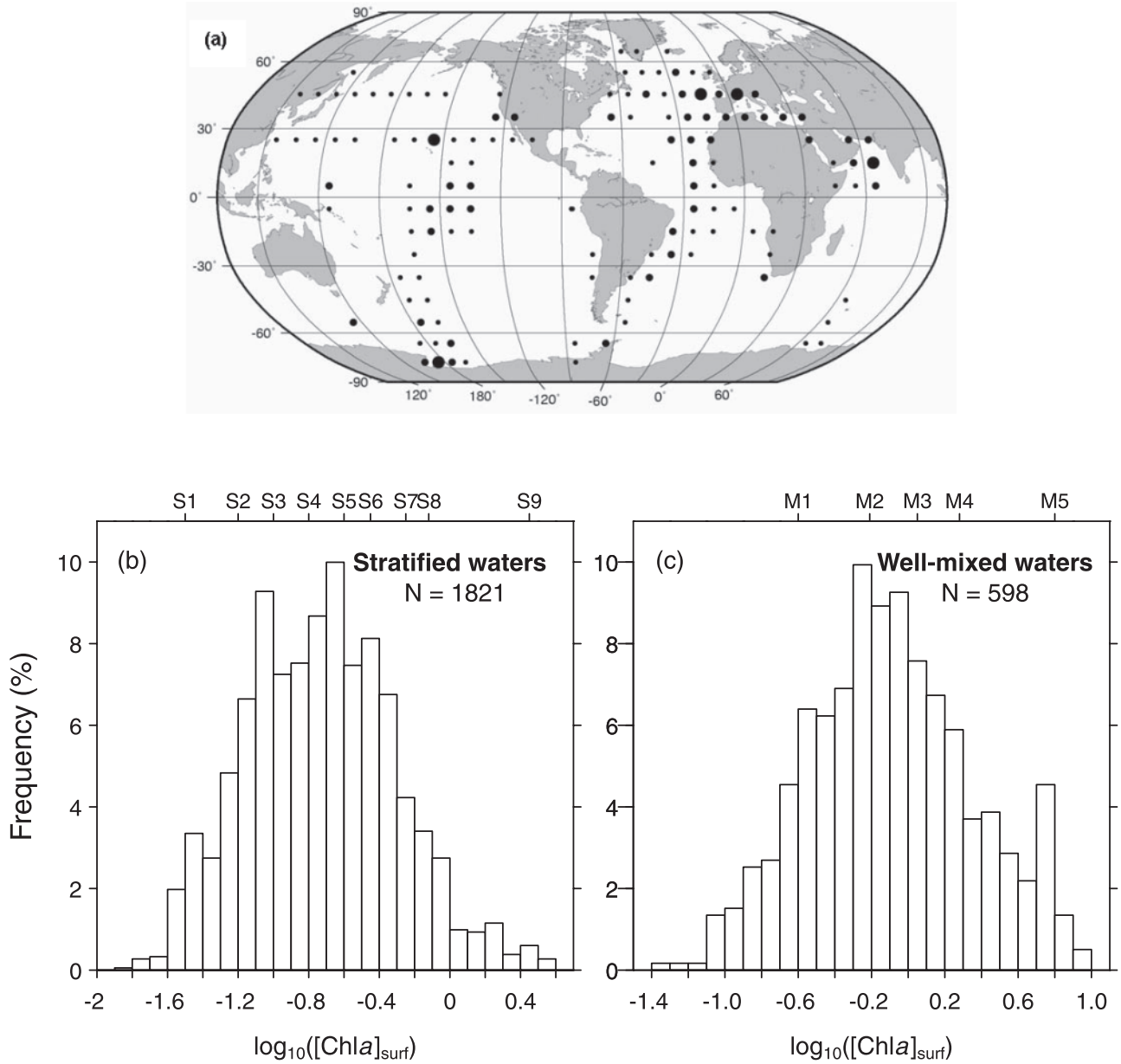

Figure 2. Distribution of the 2419 stations used in the present study. (a) Map showing the location of the stations. The size of the black dots indicates the number of stations within a 10° × 10° (latitude × longitude) sector. The small dots correspond to less than 10 stations, medium size dots correspond to 10–100 stations, and large dots correspond to more than 100 stations. Frequency distribution (% of the total items) of the data (database 1) as a function of the surface chlorophyll concentration (decimal logarithmic scale) for (b) stratified and (c) mixed waters, respectively (see text). Note the difference between Figures 2b and 2c in abscissae scales. The labels S and M refer to the categories defined in Table 3.

[11] In a first step, the quality assurance process is applied to all individual samples, those from the surface and those belonging to vertical profiles. Obviously, a rejection is needed when the set of biomarker pigments is incomplete. Then, as the detection limit of the HPLC method depends on the sensitivity of the equipment and on the filtered volumes, samples with chlorophyll *a* concentration <0.001 mg m^{-3} were rejected. For accessory pigments, concentrations below 0.001 mg m^{-3} were reset to zero. This rejection has no significant impact on the amount of useful data, because such very low pigment concentrations were normally encountered at great depths, generally beyond the depths considered in the present investigation.

[12] As shown by *Trees et al.* [2000], [Chl*a*] and the sum of the concentrations of the major accessory pigments are tightly correlated, and covary in a quasi-linear manner. The same kind of covariation is thus expected, and actually does exist, in the two databases used here (not shown). It can be used as a tool to identify and eliminate some markedly deviant data. The rejection rate in this second step of the quality assurance procedure was purposefully not severe; it eliminates outlying data when the departure exceeds three

Table 2. Diagnostic Pigments Used in the Present Study as Biomarkers and Their Taxonomic Significance [*Vidussi et al.*, 2001][a]

Diagnostic Pigments	Abbreviations	Taxonomic Significance	Phytoplankton Size Class	$\langle Chla \rangle_{Zeu}$: $\langle P \rangle_{Zeu}$	Significance Level
Fucoxanthin	Fuco	diatoms	microplankton	1.41 ± 0.02	$p < 0.001$
Peridinin	Perid	dinoflagellates	microplankton	1.41 ± 0.10	$p < 0.001$
19′-hexanoyloxyfucoxanthin	Hex-fuco	chromophytes and nanoflagellates	nanoplankton	1.27 ± 0.02	$p < 0.001$
19′-butanoyloxyfucoxanthin	But-fuco	chromophytes and nanoflagellates	nanoplankton	0.35 ± 0.15	$p = 0.02$
Alloxanthin	Allo	cryptophytes	nanoplankton	0.60 ± 0.16	$p < 0.001$
chlorophyll *b* + divinyl chlorophyll *b*	TChl*b*	green flagellates and prochlorophytes	picoplankton	1.01 ± 0.10	$p < 0.001$
Zeaxanthin	Zea	cyanobacteria and prochlorophytes	picoplankton	0.86 ± 0.09	$p < 0.001$

[a]The associated mean size class, and the corresponding $\langle Chla \rangle_{Zeu}$ to $\langle P \rangle_{Zeu}$ ratios ± SD, with their significance level are also given.

standard deviations with respect to the mean covariation relationship. Indeed, a balance must be maintained between the need to remove unwanted experimental anomalies, and the need to maintain enough data in order to respect, and account for, the possible natural variability within the observations.

[13] The last quality assurance step deals specifically with the vertical profiles. The criteria adopted here are as follows: (1) Only the profiles where the euphotic depth, Z_{eu}, was reached are kept; (2) the uppermost sample of the profile must have been collected between the surface and 10 m; and (3) each profile must include a minimal number of samples (>4), so that the shape of the vertical profiles is properly resolved. Actually, a one-by-one visual inspection of the profiles is needed to eliminate those profiles insufficiently described because of a misconceived sampling strategy or a failure in the experiment.

[14] After applying the quality assurance procedures, 2419 profiles remain in database 1, and 4238 surface samples in database 2.

2.2. Deriving Phytoplankton Community Composition From Diagnostic Pigments

[15] The HPLC pigment analysis allows the determination of a suite of pigments (usually up to 15). A first group of pigments, namely chlorophyll *a*, divinyl chlorophyll *a* and chlorophyllide *a*, is called total chlorophyll *a*, and the sum of their concentration is noted [Chl*a*]. Let us note that with this technique, chlorophyll *a* can be unambiguously separated from phaeopigments (generally insignificant in most of the open ocean waters). This was not the case in the MB89 study, where the quantity denoted C was either the chlorophyll *a* concentration or, when the acid fluorometric method was employed, the sum of chlorophyll *a* plus phaeopigments concentrations. Actually, it has been acknowledged [*Gibbs*, 1979; *Mantoura et al.*, 1997] that the fluorometric method leads to an underestimate of chlorophyll *a* and an overestimate of phaeopigments when chlorophyll *b* is present. These drawbacks disappear with the HPLC method.

[16] Beside chlorophyll a, other pigments (i.e., accessory pigments) can be determined via HPLC. Some are typical of phytoplanktonic groups and can be used as biomarkers. In order to condense the information contained within the full suite of pigments, and along the lines of previous studies [*Gieskes et al.*, 1988; *Claustre*, 1994; *Vidussi et al.*, 2001], so-called "pigment indices" are constructed with the objective of quantifying the taxonomic composition by using a minimal set of pigments. Seven major pigments are thus selected as being representative of distinct phytoplankton groups. Their taxonomic significance is summarized in Table 2 [see also *Vidussi et al.*, 2001, Table 1, and supporting references therein]. These seven pigments are fucoxanthin, peridinin, 19′-hexanoyloxyfucoxanthin, 19′-butanoyloxyfucoxanthin, alloxanthin, chlorophyll *b* and divinyl chlorophyll *b*, and zeaxanthin.

[17] *Claustre* [1994] proposed a method to quantify the relative proportion of diatoms plus dinoflagellates (collectively called "microplankton") within an algal stock, on the basis of the presence of fucoxanthin and (or) peridinin. Their proportion is represented by the ratio of concentrations

$$([\text{Fuco}] + [\text{Perid}])/\text{DP},$$

where DP represents the sum of all "diagnostic pigments" concentrations:

$$\text{DP} = [\text{Fuco}] + [\text{Perid}] + [\text{Hex-fuco}] + [\text{But-fuco}] + [\text{Allo}] + [\text{TChl}b] + [\text{Zea}].$$

[18] Later, *Vidussi et al.* [2001] extended this concept by proposing three exclusive groupings of specific pigments (among the seven significant ones), with the objective of identifying three size classes and quantifying their relative proportion. These classes are the microplankton (quantified by the ratio already introduced by *Claustre* [1994]), the nanoplankton (2–20 μm), and the picoplankton (<2 μm); these two new classes are specifically assessed by forming the (mutually exclusive) ratios:

$$([\text{Hex-fuco}] + [\text{But-fuco}] + [\text{Allo}])/\text{DP},$$

and

$$([\text{TChlb}] + [\text{Zea}])/\text{DP},$$

respectively. It should be noted (as already acknowledged by *Vidussi et al.* [2001]) that the pigment grouping here proposed does not strictly reflect the true size of phytoplankton communities. Indeed, some taxonomic pigments might be shared by various phytoplankton groups (e.g., small amounts of fucoxanthin, the main carotenoid of diatoms, may also be found in some prymnesiophytes and pelagophytes), and also some phytoplankton groups may encompass a wide size range (e.g., diatoms are sometimes observed in the nanosize range, even if generally they belong to microplankton). Notwithstanding this possible

ambiguities and the due reservation about the exact meaning of size class, this term (as well as the appellations pico, nano, micro) will be conventionally employed in what follows for the sake of brevity.

[19] These approaches provide relative proportions of classes within the phytoplanktonic assemblage (globally quantified as DP). They cannot be straightforwardly applied if the ultimate goal is a quantification of each class in terms of their concentration in chlorophyll *a*. Indeed, an equal weight given to each of the accessory pigment markers (as it is the case in the definition of DP) does not account for the natural values of the chlorophyll *a* to diagnostic pigments ratios, which in general differ from unity.

[20] *Gieskes et al.* [1988] carried out a multiple regression analysis of [Chl*a*] and the concentration of the most important accessory pigments. The partial slopes of such regressions provide the best estimates of the chlorophyll *a* to diagnostic pigments ratios (for the data set considered). The present study combines this multiple regression approach and the three specific groupings as proposed by *Vidussi et al.* [2001]. The entire database 1 (2419 profiles) is, therefore, submitted to such a multiple regression analysis (see flowchart, Figure 1), not at the level of individual samples, but after a vertical integration has been performed over the euphotic layer; in other words, the chlorophyll *a* content $\langle \mathrm{Chl}a \rangle_{\mathrm{Zeu}}$ and the seven pigment contents $\langle \mathrm{P} \rangle_{\mathrm{Zeu}}$, are considered for the regression.

[21] This regression is highly significant ($r^2 = 0.76$; $n = 2419$; $p < 0.001$). The coefficients of this regression are given in Table 2, with their standard deviation and significance level. These coefficients represent the best estimates of the seven ratios $\langle \mathrm{Chl}a \rangle_{\mathrm{Zeu}} / \langle \mathrm{P} \rangle_{\mathrm{Zeu}}$. These slopes are then used to form the weighted sum of all the diagnostic pigments concentrations, $\Sigma \mathrm{DP_w}$, expressed as:

$$\begin{aligned}\Sigma \mathrm{DP_w} = {} & 1.41[\mathrm{Fuco}] + 1.41[\mathrm{Perid}] + 1.27[\mathrm{Hex\text{-}fuco}] \\ & + 0.35[\mathrm{But\text{-}fuco}] + 0.60[\mathrm{Allo}] + 1.01[\mathrm{TChl}b] \\ & + 0.86[\mathrm{Zea}] \end{aligned} \quad (1)$$

[22] In contrast to DP, $\Sigma \mathrm{DP_w}$ represents the chlorophyll *a* concentration, which can be reconstructed from the knowledge of the concentration of the seven other pigments. The fractions of the chlorophyll *a* concentration associated with each of the three phytoplanktonic classes (f_{micro}, f_{nano} and f_{pico}) are subsequently derived according to

$$f_{micro} = (1.41[\mathrm{Fuco}] + 1.41[\mathrm{Perid}]) / \Sigma \mathrm{DP_w} \quad (2a)$$

$$f_{nano} = (1.27[\mathrm{Hex\text{-}fuco}] + 0.35[\mathrm{But\text{-}fuco}] + 0.60[\mathrm{Allo}]) / \Sigma \mathrm{DP_w} \quad (2b)$$

$$f_{pico} = (1.01[\mathrm{TChl}b] + 0.86[\mathrm{Zea}]) / \Sigma \mathrm{DP_w} \quad (2c)$$

[23] These three exclusive groupings obviously are not mathematically independent because their sum is equal to 1. The actual chlorophyll *a* concentration associated with each of the three classes is derived according to:

$$\text{micro-}[\mathrm{Chl}a] = f_{micro} \times [\mathrm{Chl}a] \quad (3a)$$

$$\text{nano-}[\mathrm{Chl}a] = f_{nano} \times [\mathrm{Chl}a] \quad (3b)$$

$$\text{pico-}[\mathrm{Chl}a] = f_{pico} \times [\mathrm{Chl}a] \quad (3c)$$

[24] A recent HPLC intercomparison exercise of pigment determination on natural samples, involving four laboratories, showed that [Chl*a*] can be determined to within an uncertainty of approximately 8% [*Claustre et al.*, 2004]; the accuracy for accessory pigments is generally less. It was shown, however, that pigment ratios (as in equations (2)) are determined with a better accuracy than individual accessory pigment concentrations (by the virtue of normalization, which cancels some analytical uncertainties). Consequently, it is believed that the use of equations (2) and (3) is very likely the most accurate approach when combining different data sources.

2.3. Using and Sorting the Data

[25] The 2419 vertical profiles (database 1) are first used to study the relationship between $[\mathrm{Chl}a]_{surf}$ and the vertically integrated chlorophyll *a* contents $\langle \mathrm{Chl}a \rangle_{\mathrm{Zeu}}$ and $\langle \mathrm{Chl}a \rangle_{1.5\mathrm{Zeu}}$, from 0 to Z_{eu} and to 1.5 Z_{eu}, respectively. Thereafter, these profiles are used to develop a parameterization of the shape of the [Chl*a*] profiles according to the trophic status, which is conventionally depicted by $[\mathrm{Chl}a]_{surf}$. This phase of the present work aims at testing the MB89 results against an entirely different database.

[26] In a second phase, the same database is split into two subsets by using a random sorting. The first subset comprises 80% of the vertical profiles (1936 stations), which are statistically analyzed in view of deriving the vertical average profiles of fractional [Chl*a*] (namely the micro-[Chl*a*], nano-[Chl*a*], and pico-[Chl*a*] profiles), and then of proposing a parameterization for these profiles. The remaining profiles (483 stations) are used to validate the proposed parameterization.

3. Methods

3.1. Relating Near-Surface and Vertically Integrated Chlorophyll *a* Contents

[27] The procedure (as in MB89) first requires that the stations in well-mixed waters and in stratified waters be identified and considered separately. This sorting is made according to the ratio between the depth of the euphotic layer, Z_{eu}, and the mixed layer depth, Z_m. The station is assumed to be in well-mixed waters when $Z_{eu}/Z_m < 1$, and in a stratified water column if $Z_{eu}/Z_m > 1$. The euphotic depth (Z_{eu}), generally not measured, as well as the mixed layer depth (Z_m), were not available. Thus the euphotic depth was inferred from the [Chl*a*] vertical profile, using a bio-optical model for light propagation. In MB89, the model of *Morel* [1988] was used. This model has been recently revised [*Morel and Maritorena*, 2001], yielding minor changes in Z_{eu} (actually slightly increased Z_{eu} values in

Table 3. Trophic Categories Defined With Respect to the Chlorophyll *a* Concentration Within the Surface Layer, $[Chla]_{surf}$, and the Associated Parameters[a]

	Stratified Waters									Mixed Waters				
	S1	S2	S3	S4	S5	S6	S7	S8	S9	M1	M2	M3	M4	M5
$[Chla]_{surf}$ range, mg m^{-3}	<0.04[b]	0.04–0.08	0.08–0.12	0.12–0.2	0.2–0.3	0.3–0.4	0.4–0.8	0.8–2.2	2.2–4[c]	<0.4[d]	0.4–0.8	0.8–1	1–4	>4[e]
Number of profiles	109	268	269	320	287	180	260	110	18	155	153	53	182	55
Average $[Chla]_{surf}$, mg m^{-3}	0.032	0.062	0.098	0.158	0.244	0.347	0.540	1.235	2.953	0.244	0.592	0.885	1.881	6.320
	(0.005)	(0.012)	(0.012)	(0.023)	(0.030)	(0.028)	(0.106)	(0.403)	(0.520)	(0.092)	(0.112)	(0.051)	(0.753)	(2.916)
Average $\overline{Chla}_{Zeu}$, mg m^{-3}	0.0910	0.151	0.185	0.250	0.338	0.410	0.578	1.206	2.950	0.280	0.591	0.872	2.059	7.574
	(0.025)	(0.067)	(0.088)	(0.144)	(0.152)	(0.153)	(0.229)	(0.526)	(1.191)	(0.130)	(0.175)	(0.189)	(0.996)	(3.700)
Average $\langle Chla \rangle_{Zeu}$, mg m^{-2}	10.54	14.15	15.98	18.79	22.09	24.70	29.72	44.05	71.98	19.90	30.27	37.57	58.64	120.00
	(1.84)	(3.31)	(3.29)	(4.08)	(4.99)	(4.64)	(5.88)	(10.46)	(15.28)	(4.70)	(4.73)	(4.44)	(15.30)	(26.75)
Average $\langle Chla \rangle_{1.5\ Zeu}$, mg m^{-2}	18.27	22.13	24.74	27.19	29.42	31.83	38.22	58.18	101.33	28.46	40.22	51.49	85.42	178.37
	(3.97)	(5.18)	(6.35)	(8.29)	(8.58)	(8.76)	(9.57)	(19.9)	(26.59)	(7.52)	(8.17)	(8.13)	(26.80)	(44.55)
Average Z_{eu}, m	119.1	99.9	91.0	80.2	70.3	63.4	54.4	39.8	26.1	77.1	53.2	44.0	31.5	16.9
	(12.2)	(15.4)	(11.8)	(12.6)	(11.9)	(9.3)	(8.2)	(8.0)	(4.5)	(14.3)	(6.8)	(4.6)	(6.8)	(2.4)

[a]These parameters are derived from the calculations involving the complete database 1 and are presented as averages and standard deviations (the latter shown in parentheses).
[b]Minimum value 0.015 mg m^{-3}.
[c]Maximum value 3.97 mg m^{-3}.
[d]Minimum value 0.047 mg m^{-3}.
[e]Maximum value 23.9 mg m^{-3}.

oligotrophic waters). This revised model is used in the present study. For the mixed layer depths, the values were extracted for the appropriate month and geographic location from the World Ocean Atlas [*Monterey and Levitus*, 1997]. Another recent mixed layer depth climatology [*de Boyer Montégut et al.*, 2004] was also used with no significant impact on the partitioning between mixed and stratified waters (2% of the total number of stations changed their categorization).

[28] The statistical analysis is performed on the basis of two dimensionless quantities. A dimensionless depth, ζ, is introduced, which is obtained by dividing the geometrical depth, z, by Z_{eu}:

$$\zeta = z/Z_{eu} \tag{4}$$

[29] Even when scaled with respect to ζ, the various profiles with differing pigment content cannot be straightforwardly compared. Another normalization is needed, which consists of considering dimensionless chlorophyll *a* concentrations, denoted $c(\zeta)$, defined as:

$$c(\zeta) = [Chla(\zeta)]/\overline{Chla}_{Zeu}. \tag{5}$$

where $\overline{Chla}_{Zeu}$ is the average concentration within the euphotic layer, namely,

$$\overline{Chla}_{Zeu} = (Z_{eu})^{-1} \int_0^{Zeu} [Chla(z)]dz, \tag{6}$$

which, in practice, is computed by a trapezoidal integration, on the basis of the discrete data. After this double normalization has been applied, the dimensionless $c(\zeta)$ profiles can be pooled together and compared, regardless of their absolute magnitudes.

[30] In anticipation of further statistical analyses of the shape of the profiles, it is convenient to describe these profiles with regularly spaced $c(\zeta)$ values. This is obtained by linear interpolation between the actual data, with an increment in ζ equal to 0.1. This interpolation is extended beyond Z_{eu} ($\zeta > 1$), whenever possible. The rationale for this extension lies in the frequent occurrence of a deep chlorophyll maximum in the vicinity of, or slightly beyond, Z_{eu}, particularly in oligotrophic waters [*Letelier et al.*, 2004].

[31] The dimensionless $c(\zeta)$ profiles are then sorted according to their absolute $[Chla]_{surf}$ value into different "trophic categories," which are defined by successive intervals within the $[Chla]_{surf}$ continuum. These intervals and their limits are given in Table 3. For each category, an average $c(\zeta)$ profile is computed, with its standard deviation (see Figures S1–S8 in auxiliary material).

3.2. Parameterization of the Chlorophyll *a* Vertical Profiles

[32] The regular change in shape of the chlorophyll *a* profiles as a function of $[Chla]_{surf}$ allows its parameterization. In MB89, the average dimensionless profile of each trophic category was modeled by using a generalized Gaussian profile [*Lewis et al.*, 1983], superimposed onto a constant background concentration. A slightly modified version of this model is introduced here. Its purpose is to

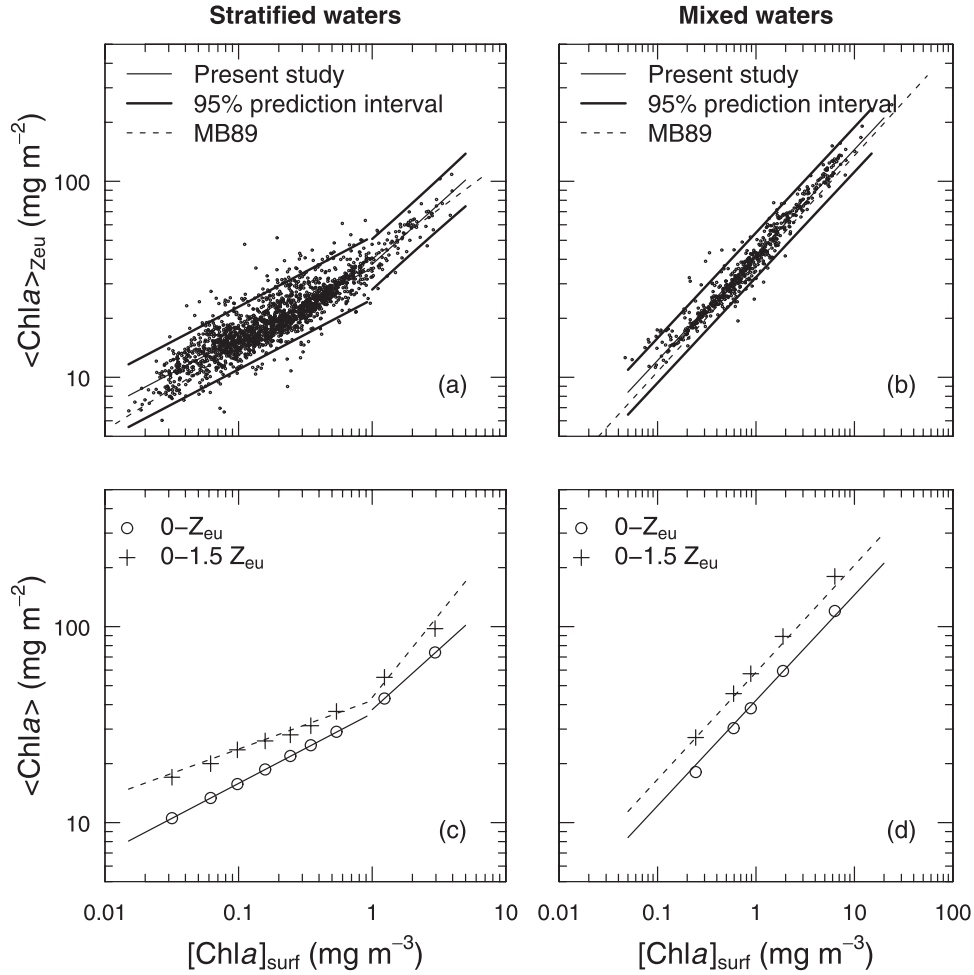

Figure 3. Integrated Chl*a* content over the euphotic layer, $\langle \mathrm{Chl}a \rangle_{\mathrm{Zeu}}$, plotted as a function of the surface Chl*a* concentration, $[\mathrm{Chl}a]_{\mathrm{surf}}$, for (a) stratified waters and (b) mixed waters. Solid lines represent the results of the regression according to equation (8) and Table 4, and bold lines delimit the 95% prediction interval. The dashed lines reproduce the regression line of MB89. (c) Stratified waters and (d) mixed waters, in which open dots and crosses represent $\langle \mathrm{Chl}a \rangle_{\mathrm{Zeu}}$ and $\langle \mathrm{Chl}a \rangle_{1.5\mathrm{Zeu}}$, respectively. They have been computed for each trophic category, by using the modeled profiles (section 4.3); they are compared to the results of the regression analyses: Solid lines are reproduced from Figures 3a and 3b, and dashed lines are from the regression between $\langle \mathrm{Chl}a \rangle_{1.5\mathrm{Zeu}}$ and $[\mathrm{Chl}a]_{\mathrm{surf}}$ (Table 4).

account for the fact that surface chlorophyll values generally exceed the deepest values (beyond Z_{eu} or more), which is incompatible with a constant background. The constant background is, therefore, simply replaced by a linear decrease with a slope, s, starting from the surface value, C_b. The generic equation (with 5 parameters) is written as

$$c(\zeta) = C_b - s\zeta + C_{max} \exp\left\{-[(\zeta - \zeta_{max})/\Delta\zeta]^2\right\}, \qquad (7)$$

where C_{max} represents the maximum concentration, ζ_{max} the depth at which this maximum occurs, and $\Delta\zeta$ depicts the width of the peak.

4. Results

4.1. Column-Integrated and Surface Chlorophyll *a*

[33] In MB89, a distinction was made between the arithmetic mean concentration over the first penetration depth, $Z_{eu}/4.6$ [*Gordon and McCluney*, 1975] and the weighted concentration within the same layer (denoted C_{sat}). This distinction was shown to be useless. Here, a unique quantity, denoted $[\mathrm{Chl}a]_{\mathrm{surf}}$, is used and represents the arithmetic average over the first penetration depth. The chlorophyll *a* content integrated over the euphotic zone, $\langle \mathrm{Chl}a \rangle_{\mathrm{Zeu}}$, is studied as a function of $[\mathrm{Chl}a]_{\mathrm{surf}}$. The log-log plots of these quantities (Figure 3) suggest that nonlinear relationships of the form

$$\langle \mathrm{Chl}a \rangle_{\mathrm{Zeu}} = A[\mathrm{Chl}a]^B_{\mathrm{surf}} \qquad (8)$$

are appropriate, where the exponent B is notably below unity. Stratified and mixed waters are studied separately.

[34] In the plot for stratified regimes (Figure 3a), a change in the slope (already noted in MB89) distinctly occurs around $[\mathrm{Chl}a]_{\mathrm{surf}} \approx 1$ mg m^{-3}, so two separate regression analyses on each side of this threshold are carried out

Table 4. Statistical Relationships Between the Average Chl*a* Concentration Within the Surface Layer, $[Chla]_{surf}$, and the Chl*a* Integrated Content Within the Euphotic Layer, $\langle Chla \rangle_{Zeu}$, and Within the 0–1.5 Z_{eu} Layer, $\langle Chla \rangle_{1.5\ Zeu}$[a]

Present Study	MB89
Stratified Waters	
For $[Chla]_{surf} \leq 1$ mg m^{-3}	
$\langle Chla \rangle_{Zeu} = 36.1[Chla]_{surf}^{0.357}$[b], n = 1743, $r^2 = 0.73$, $p < 0.001$	$\langle Chla \rangle_{Zeu} = 38.0[Chla]_{surf}^{0.425}$
$\langle Chla \rangle_{1.5Zeu} = 42.0[Chla]_{surf}^{0.248}$[b], n = 1129, $r^2 = 0.43$, $p < 0.001$	
For $[Chla]_{surf} > 1$ mg m^{-3}	
$\langle Chla \rangle_{Zeu} = 37.7[Chla]_{surf}^{0.615}$[b], n = 78, $r^2 = 0.70$, $p < 0.001$	$\langle Chla \rangle_{Zeu} = 40.2[Chla]_{surf}^{0.507}$
$\langle Chla \rangle_{1.5Zeu} = 43.5[Chla]_{surf}^{0.847}$[b], n = 59, $r^2 = 0.68$, $p < 0.001$	
Mixed Waters	
$\langle Chla \rangle_{Zeu} = 42.1[Chla]_{surf}^{0.538}$[b], n = 598, $r^2 = 0.95$, $p < 0.001$	$\langle Chla \rangle_{Zeu} = 38.0[Chla]_{surf}^{0.551}$
$\langle Chla \rangle_{1.5Zeu} = 58.5[Chla]_{surf}^{0.546}$[b], n = 489, $r^2 = 0.90$, $p < 0.001$	

[a]The relationships obtained by MB89 are also reproduced. $[Chla]_{surf}$ values are given in mg m^{-3}, and $\langle Chla \rangle_{Zeu}$ and $\langle Chla \rangle_{1.5\ Zeu}$ values are given in mg m^{-2}.
[b]See equation (8) in text.

(Table 4). In the domain below the threshold, the scatter of the data points is more important than above, and reflects the variability partly due to the existence of a deep chlorophyll maximum typical of oligotrophic conditions. In mixed waters, the log-log plot of $\langle Chla \rangle_{Zeu}$ versus $[Chla]_{surf}$ (Figure 3b) shows a unique linear trend, a steeper slope (Table 4), and a lower scatter in the data points, as a result of the rather homogenous pigment distribution.

[35] The present results are very consistent with, and independently confirm, those of MB89 (shown as dashed lines in Figure 3). The factor and exponent values (A and B) arrived at are slightly differing from those in MB89 (see Table 4), but the differences are statistically insignificant. The closeness of the exponents for mixed waters and for stratified waters as soon as $[Chla]_{surf} > 1$ mg m^{-3} (0.538 versus 0.615, respectively; Table 4) emphasizes that the algal biomass in eutrophic conditions remains rather uniformly distributed within the euphotic layer, essentially as a consequence of its reduced thickness.

[36] Because it is recognized that an important phytoplanktonic biomass is often present below the euphotic depth, the study is complemented by considering a thicker layer, extended down to 1.5 Z_{eu}. The column content integrated over this layer, $\langle Chla \rangle_{1.5\ Zeu}$, is regressed against $[Chla]_{surf}$, as above. The corresponding parameters A and B are provided in Table 4 (see also Figures 3c and 3d).

4.2. Chlorophyll *a* Vertical Profiles

[37] On the basis of increasing $[Chla]_{surf}$ values, the vertical chlorophyll *a* profiles have been sorted into nine trophic categories for the stratified waters, from S1 to S9, and five for the mixed waters, from M1 to M5 (instead of seven and two in MB89, respectively). This more detailed categorization was possible because lower surface concentrations (<0.04 for S1) were present in sufficient number, and the populated middle range of concentrations could be resolved into more classes (see Table 3 and Figures 2b and 2c). At the extreme (high values) end, the S8, S9, and M5 classes, contain significantly less data.

4.2.1. Stratified Waters

[38] In these waters, the shape of the average dimensionless profiles (down to $\zeta = 2$) exhibits a remarkably regular change along the trophic status (Figure 4a). When $[Chla]_{surf}$ increases, the change in shape is characterized by (1) a smooth ascent of the chlorophyll *a* maximum, from a depth equal to about Z_{eu} for S1, up to the near-surface for S9; and (2) a regular decrease in the relative magnitude of the deep maximum with respect to the background. This change is very similar to that described in MB89 (their categories a to g, for stratified regimes).

[39] These mean profiles are used in conjunction with equation (7). The fitting procedure (a Newton-type algorithm from the library of the R software [*R Development Core Team*, 2004]) allows the five parameters involved in equation (7) to be derived for each category from S1 to S9 (Table 5). With these parameters, the modeled profiles are computed by using the average $[Chla]_{surf}$ value of each category (Table 3); they compare well with the average profiles (Figure 4b). The regular change in shape suggests that the parameterization can be used in a continuous fashion. For any $[Chla]_{surf}$ value, the appropriate five parameters can be linearly interpolated between the two categories (depicted by their $[Chla]_{surf}$ values in Table 3) that bracket the actual value (note that this interpolation was made through polynomials in MB89).

[40] The dimensionless profiles can be restored to their physical values (i.e., ''rescaled'' in concentration and depth) by reintroducing the actual Z_{eu} and $\overline{Chla}_{Zeu}$ values. Both are retrieved using equation (8), linking $\langle Chla \rangle_{Zeu}$ to $[Chla]_{surf}$, and Z_{eu} to $\langle Chla \rangle_{Zeu}$ [*Morel and Maritorena*, 2001, equation (6)]. These restored profiles (Figures 4c and 4d) provide an undistorted visualization of the physical profiles and of their change when the surface concentration changes. For the whole range, when $[Chla]_{surf}$ increases from about 0.03 to 3.0 mg m^{-3} (S1 to S9), the chlorophyll *a* maximum increases from 0.17 to 3 mg m^{-3}, whereas Z_{eu} decreases from about 120 to 25 m.

[41] A quantitative comparison of the present parameterization and that of MB89 has been performed by using a synthetic set of $[Chla]_{surf}$ values. The results show that the profiles generated by both parameterizations are in general fully consistent (see Figure S9 in auxiliary material).

4.2.2. Vertically Mixed Waters

[42] In this regime, the average dimensionless chlorophyll *a* profiles (Figure 5a) show a rather featureless shape: no maximum (except for M1), a constant concentration which remains approximately equal (to within ±10%) to the average concentration within the euphotic layer, and finally a systematic decrease in concentration (by about a

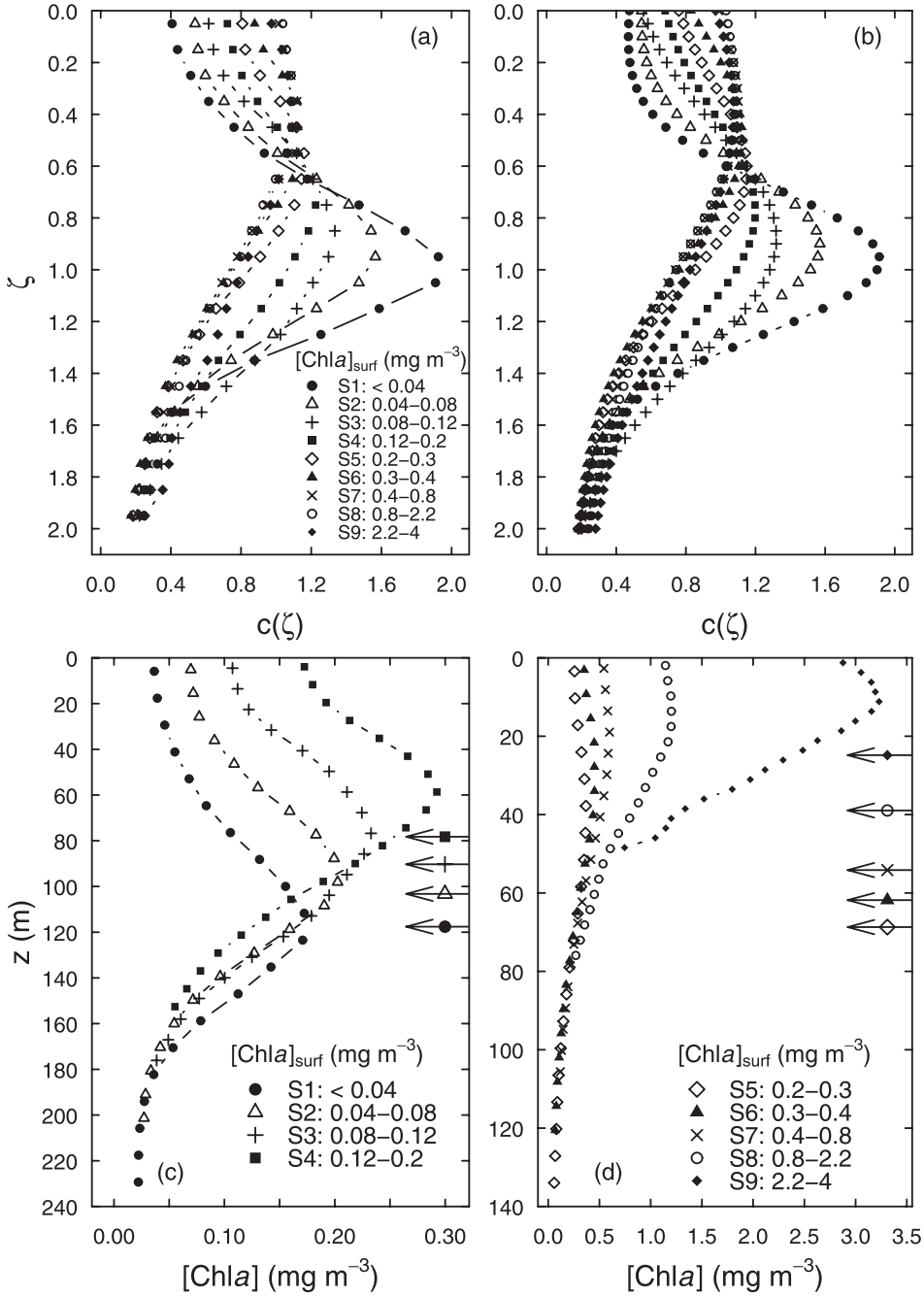

Figure 4. Chl*a* vertical profiles for stratified waters: (a) the average dimensionless Chl*a* profiles obtained for each trophic category, (b) the corresponding modeled dimensionless Chl*a* profiles, (c) the rescaled Chl*a* profiles for categories S1 to S4, and (d) the rescaled Chl*a* profiles for categories S5 to S9. For each of the rescaled profiles, the position of Z_{eu} is indicated by an arrow identified by the symbol corresponding to its trophic category. Note that the standard deviations not shown are available for each category and displayed on separate figures in auxiliary material (Figures S1–S8).

factor of 2) between Z_{eu} and 2 Z_{eu}. The values observed at 2 Z_{eu}, however, are still about 40% of the average value within the euphotic column, (instead of less than 20% in stratified waters), which is a signature of the deep vertical mixing. The physically rescaled profiles (Figures 5b and 5c) show that [Chl*a*] varies from approximately 0.2 to about 5 mg m^{-3}. The first situation with low concentrations (M1) is actually encountered during the winter vertical mixing in the North Atlantic, and also in the Mediterranean Sea. The M5 category essentially (75%) includes observations in the Ross Sea, with a mixed layer extending deeper (40–80 m) than the euphotic layer (20 m). Actual surface [Chl*a*] range from 4 to about 30 mg m^{-3}. The average profile exhibits a weakly marked chlorophyll maximum (+15% compared to the surface value). The present results and those in MB89 for these mixed regimes agree remarkably well.

Table 5. Values of the Five Parameters to be Used in Equation (7), Obtained for the Average Dimensionless Vertical Profiles of Chl*a*, Micro-Chl*a*, Nano-Chl*a*, and Pico-Chl*a*, for Each Trophic Class of the Stratified Waters (S1 to S9)

Trophic	Chl*a*					Micro-Chl*a*					Nano-Chl*a*					Pico-Chl*a*				
Class	C_b	s	C_{max}	ζ_{max}	$\Delta\zeta$	C_b	s	C_{max}	ζ_{max}	$\Delta\zeta$	C_b	s	C_{max}	ζ_{max}	$\Delta\zeta$	C_b	s	C_{max}	ζ_{max}	$\Delta\zeta$
S1	0.471	0.135	1.572	0.969	0.393	0.036	0.020	0.122	1.012	0.532	0.138	0.033	0.764	0.980	0.451	0.222	0.114	0.906	0.970	0.352
S2	0.533	0.172	1.194	0.921	0.435	0.071	0.020	0.173	0.885	0.406	0.129	0.014	0.589	0.899	0.454	0.242	0.109	0.627	0.977	0.427
S3	0.428	0.138	1.015	0.905	0.630	0.076	0.021	0.126	0.835	0.424	0.142	0	0.463	0.872	0.526	0.254	0.099	0.437	0.969	0.634
S4	0.570	0.173	0.766	0.814	0.586	0.071	0.021	0.160	0.776	0.546	0.192	0.037	0.400	0.782	0.535	0.271	0.100	0.255	0.858	0.637
S5	0.611	0.214	0.676	0.663	0.539	0.145	0.050	0.163	0.700	0.479	0.188	0.055	0.418	0.650	0.640	0.159	0.052	0.176	0.574	0.650
S6	0.390	0.109	0.788	0.521	0.681	0.173	0.044	0.161	0.600	0.508	0.331	0.132	0.294	0.501	0.516	0.176	0.071	0.129	0.458	0.626
S7	0.569	0.183	0.608	0.452	0.744	0.237	0.077	0.158	0.521	0.543	0.201	0.084	0.350	0.402	0.724	0.009	0	0.251	0.239	0.943
S8	0.835	0.298	0.382	0.512	0.625	0.331	0.105	0.278	0.451	0.746	0.227	0.081	0.198	0.181	0.690	0.094	0.040	0.109	0.187	0.618
S9	0.188	0	0.885	0.378	1.081	0.891	0.302	0.000	0.277	1.014	0.171	0	0.088	0.375	0.352	0.051	0.023	0.000	0.052	0.417

4.3. Coherence Between the Chlorophyll *a* Profiles and the Column-Integrated Content

[43] The two previous and independent statistical analyses have related the surface chlorophyll *a* first to the column-integrated content (section 4.1), and secondly to the vertical profiles (section 4.2). From the second study, it was possible to extract and then parameterize typical profiles as a function of $[\text{Chl}a]_{surf}$. The internal consistency of the two approaches is easily tested. After being scaled in physical units, the modeled profiles (S1 to S9, and M1 to M5) can be vertically integrated down to Z_{eu}, and 1.5 Z_{eu}, to provide $\langle \text{Chl}a \rangle_{Zeu}$ and $\langle \text{Chl}a \rangle_{1.5\ Zeu}$. The corresponding values are plotted on Figures 3c and 3d, in a format similar to that used for the field data. The comparison with the regression lines reproduced from Figures 3a and 3b shows the agreement between the two statistical approaches is excellent regarding the column content within the euphotic layer. When considering the extended euphotic layer (1.5 Z_{eu}), the vertically integrated biomass is increased by 25% in eutrophic stratified waters, and by more than 60% in oligotrophic waters, as a logical consequence of the inclusion of the deep chlorophyll maximum. In mixed waters, the increase is of the order of 40%, regardless of the trophic level.

4.4. Microplankton, Nanoplankton, and Picoplankton Respective Contributions in Stratified Waters

4.4.1. Column-Integrated Contents

[44] The fraction (80%) of database 1 is now used to study the vertical distribution of the phytoplankton composition (Figure 1). By using the detailed pigment composition together with equations (2) and (3), the fractional [Chl*a*] related to each of the three size classes, can be computed at each depth and for each profile. The profiles are then vertically integrated down to 1.5 Z_{eu}, and averaged within each trophic category (S1 to S9). These fractional column-integrated chlorophyll *a* are shown (Figure 6a) as percentages of $\langle \text{Chl}a \rangle_{1.5Zeu}$ (all populations merged), or (Figure 6b) as absolute values (as mg m^{-2}). Both quantities are plotted as a function of the central $[\text{Chl}a]_{surf}$ values of each category.

[45] In the most oligotrophic waters (S1), the picoplankton and nanoplankton biomasses are almost of equal importance, i.e., about 45% each of the total biomass (Figure 6a). In contrast, microplankton dominate (75%) in eutrophic waters (S9), whereas nanoplankton represent only 21% and picoplankton represent 4% of $\langle \text{Chl}a \rangle_{1.5\ Zeu}$. In mesotrophic waters, with $[\text{Chl}a]_{surf}$ around 0.3 mg m^{-3}, nanoplankton dominate (50%), while picoplankton and microplankton account for the remainder in similar proportions (25% each). When the absolute contents (as mg m^{-2}, Figure 6b) are considered, a simple picture emerges; the increase in the chlorophyll *a* values along the trophic continuum (two orders of magnitude in $[\text{Chl}a]_{surf}$) is essentially caused by the increase in the microplankton biomass. Meanwhile the picoplankton population appears as a rather constant background (approximately 5 mg m^{-2}), whereas the nanoplankton population experiences an increase (actually a tripling) from oligotrophic to eutrophic conditions.

[46] The changing composition of phytoplankton assemblages along with the surface chlorophyll concentration, agrees with ecological knowledge and previous microscopic observations [*Malone*, 1980; *Chisholm*, 1992]. For instance, it is known that picoplankton predominate in oligotrophic environments (e.g., subtropical gyres), and diatoms in eutrophic zones (e.g., in upwelling areas), in coherence with the present findings. The present quantitative analysis also reveals the ubiquity and relative stability around 45% (except in eutrophic waters) of the nanoplankton compartment, in keeping with the omnipresence of Hex-fuco [*Ondrusek et al.*, 1991; *Vidussi et al.*, 2001], a typical marker of these species.

[47] When the relative proportions are separately analyzed for the surface layer (Figure 6c), and compared to those recorded for the 0–1.5 Z_{eu} layer (Figure 6a), notable differences are seen for the S2–S4 categories: the picoplankton contribution is slightly enhanced near the surface, at the expense of the nanoplankton.

4.4.2. Vertical Profiles

[48] The average dimensionless profiles of chlorophyll *a* associated to the microplankton, nanoplankton, and picoplankton classes are computed by introducing the values produced by equations (3a)–(3c) into equation (6), and by keeping the denominator unchanged (i.e., $\overline{\text{Chl}a}_{Zeu}$, corresponding the three populations merged). These profiles for stratified waters are shown in Figures 7a–7c. Their regular change according to the trophic regime hold much in common with those of the total population (Figure 4a), at least for the picoplankton and nanoplankton. For these size classes, a distinct deep maximum occurs and becomes shallower and smoother as $[\text{Chl}a]_{surf}$ increases. This maximum is slightly sharper for picoplankton than for nanoplankton in most oligotrophic waters (S1 to S4). For the most oligotrophic category (S1), the peak values for the

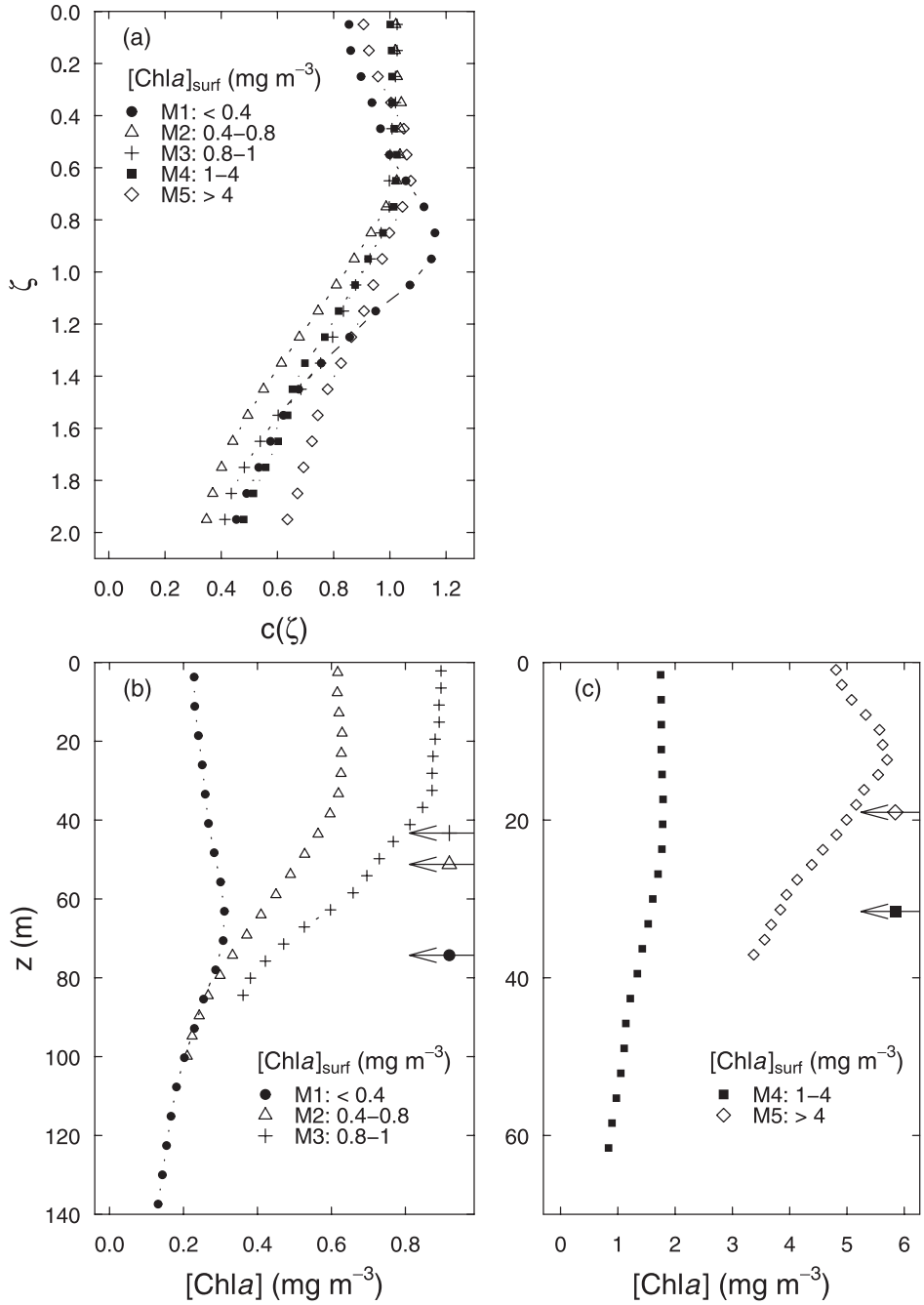

Figure 5. Chl*a* vertical profiles for mixed waters: (a) the average dimensionless Chl*a* profiles obtained for each trophic category and the rescaled Chl*a* profiles for (b) categories M1 to M3 and (c) categories M4 and M5. For each of the rescaled profiles, the position of Z_{eu} is indicated by an arrow identified by the symbol corresponding to its trophic category. Note that the standard deviations not shown are available for each category and displayed on separate figures in auxiliary material (Figures S1–S8).

picoplankton and nanoplankton are each almost equal to $\overline{\text{Chl}a}_{Zeu}$ (normalized values close to 1), which is possible because the (total) chlorophyll *a* maximum is about twice $\overline{\text{Chl}a}_{Zeu}$ (Figure 4a). Globally, the deep chlorophyll *a* maximum for these waters is almost entirely made up of picoplankton and nanoplankton assemblages, in agreement with the column-integrated contents (see above); the contribution of the microplankton is extremely low (<0.2 $\overline{\text{Chl}a}_{Zeu}$), with rather featureless profiles (Figure 7a).

[49] In eutrophic conditions (S8 and S9), a smooth microplankton maximum tends to develop near the surface, while the nanoplankton and picoplankton chlorophyll *a* profiles become uniform, with low relative values. For mesotrophic regimes, (with $[\text{Chl}a]_{surf} \approx 0.2–0.5$ mg m^{-3}; see S5 and S6), nanoplankton are predominant everywhere in the water column.

[50] The parameterization of the (fractional) chlorophyll *a* profiles for the three phytoplanktonic groups is made as above (according to equation (7)). The profiles recon-

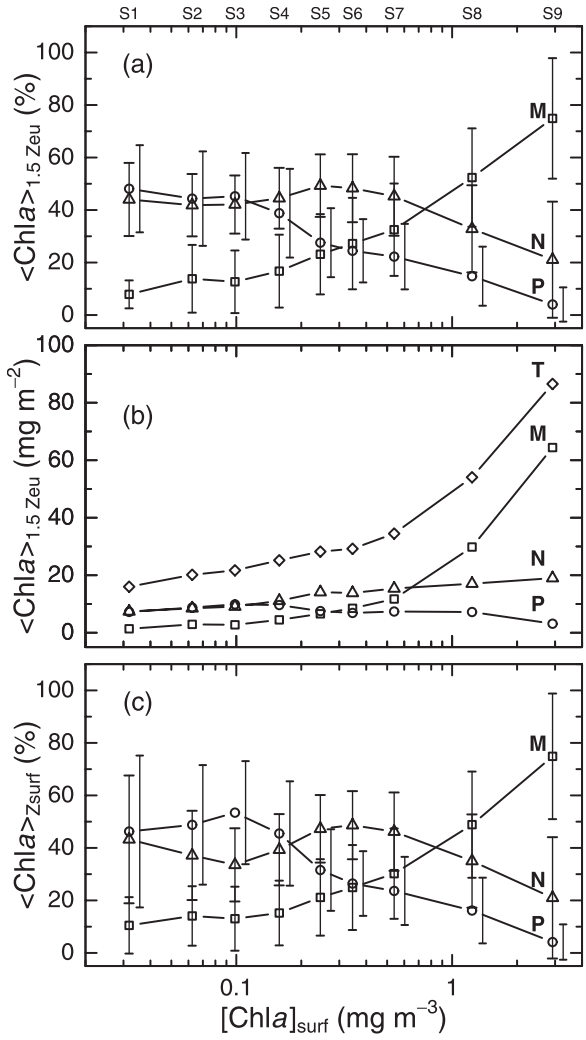

Figure 6. Composition of the phytoplankton community as a function of [Chl*a*]$_{surf}$ for stratified waters. (a) Average proportions (%) of micro-Chl*a*, nano-Chl*a* and pico-Chl*a*, within the 0–1.5 Z_{eu} layer, (b) average contents (mg m^{-2}) of micro-[Chl*a*], nano-[Chl*a*], pico-[Chl*a*], and [Chl*a*] integrated over the 0–1.5 Z_{eu} layer, and (c) average proportions (%) of micro-Chl*a*, nano-Chl*a* and pico-Chl*a*, within the surface layer only. The vertical bars represent ±1 SD around the mean values. The labels M, N, and P refer to microplankton, nanoplankton and picoplankton, respectively.

structed with the appropriate parameters (Table 5) are displayed in Figures 7d–7f. They reproduce fairly well the average profiles as derived from the statistical analysis. The same profiles, rescaled in their physical concentration and depth values, are displayed in Figure 8. The absolute magnitude of the picoplankton peaks remains about the same (0.09–0.11 mg m^{-3}) for the first four classes (S1 to S4), in contrast to the nanoplankton peaks which steadily increase (from 0.08 to 0.14 mg m^{-3}).

4.5. Microplankton, Nanoplankton, and Picoplankton Respective Contributions in Well-Mixed Waters

4.5.1. Global Ocean

[51] About one third of the stations in mixed waters (184 over 479) were located in the Southern Ocean (south of 60°S). These data are examined separately for reasons explained below. The 295 remaining stations are analyzed as above, by keeping the same categorization (M1 to M5).

[52] The integrated contents (over 1.5 Z_{eu}) of micro-[Chl*a*], nano-[Chl*a*], and pico-[Chl*a*], expressed as a percentage of the total content, are displayed as a function of [Chl*a*]$_{surf}$ in Figure 9a (to be compared with Figure 6a). The respective proportions of the three classes are similar in mixed and stratified waters. In both cases, the contribution of the microplankton increases along with [Chl*a*]$_{surf}$, while the contributions of nanoplankton and picoplankton decrease. The major difference lies in a lower contribution of picoplankton in oligotrophic mixed waters (30% versus 40% in stratified waters).

[53] As expected from the chlorophyll *a* profiles (Figure 5b), the individual profiles of picoplankton, nanoplankton, and microplankton (Figures 10a–10c) are also rather featureless; they are essentially uniform within the euphotic layer, and decrease from $\zeta = 1$ to $\zeta = 2$. The size composition bears some resemblance with that observed in stratified waters. Indeed, in low-chlorophyll waters ([Chl*a*]$_{surf}$ < 0.4 mg m^{-3}), the microplankton fraction is at its minimum (20% of $\overline{\text{Chl}a_{Zeu}}$), while the picoplankton and nanoplankton dominate (with a smooth peak near $\zeta = 0.8$). The latter is relatively more abundant (50% versus 30%), in contrast to what happens in stratified waters. In eutrophic regimes, the microplankton fraction largely dominates (more than 80%), and this dominance is similar to what was described for stratified waters (Figure 6a). Note that in stratified waters with high chlorophyll content, the depth of the euphotic zone is reduced to such a point that the distinction between stratified and mixed waters tends to vanish.

4.5.2. Particular Case of the Southern Ocean (of the Ross Sea?)

[54] About 80% of the data in Antarctic waters originate from the Ross Sea, therefore the results presented below may not be representative of the whole Southern Ocean. Mixed waters in this sector are dealt with separately, because a preliminary analysis of the data set has shown that a Hex-fuco (prymnesiophytes) increase is usually observed during bloom periods, in contrast to temperate latitudes where the blooms are generally associated with a Fuco (diatoms) increase. More generally, the partition of the mixed waters data into two subsets (global and southern) is consistent with a recent body of literature which emphasizes the particular bio-optical status [*Stramska et al.*, 2003; *Cota et al.*, 2003] and taxonomic compositions [*Sathyendranath et al.*, 2001] of polar waters.

[55] This partition appears a posteriori justified by the comparative examination of Figures 9a and 9b, showing that, in southern waters, the relative roles of the three phytoplankton groups differ significantly. Actually, the picoplankton biomass, which never exceeds 10% of the total chlorophyll *a* content, is distinctly lower in southern waters than in any other areas. Microplankton dominate at low [Chl*a*]$_{surf}$ and decrease to the benefit of nanoplankton when [Chl*a*]$_{surf}$ increases. In reality, what is called microplankton is (maybe small) diatoms, whereas the nanoplankton class refers to prymnesiophytes (probably colonial *Phaeocystis*). At [Chl*a*]$_{surf}$ > 2 mg m^{-3}, prymnesiophytes represent up to 60 to 80% of the biomass in southern waters, while diatoms represent 60 to 90% of the biomass in

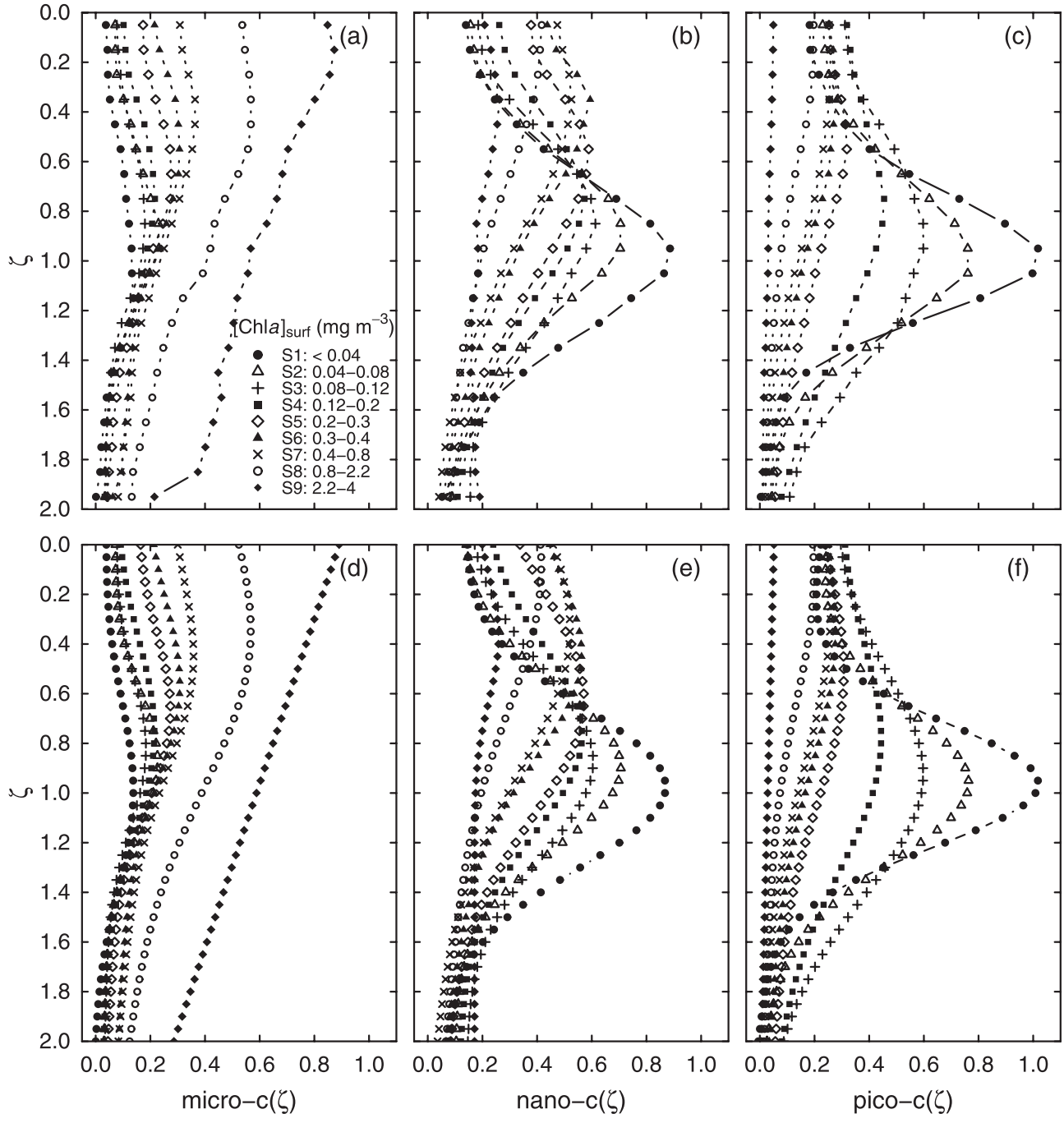

Figure 7. (a–c) Average and (d–f) modeled dimensionless vertical profiles of micro-Chl*a*, nano-Chl*a* and pico-Chl*a* in stratified waters. Trophic categories are the same as in Figure 5.

temperate waters. These features are consistent with diverse field observations, which indicate that *Phaeocystis* blooms appear, in the Ross Sea, in unstable conditions, whereas diatom blooms would occur when stratification prevails [*Goffart et al.*, 2000; *Boyd*, 2002; *Arrigo et al.*, 2003]. According to additional observations in other southern sectors, phytoplankton blooms can be dominated either by Hex-containing species (*Phaeocystis spp*., other prymnesiophytes, and cryptophytes) or by diatoms [*Moline and Prézelin*, 1996; *Claustre et al.*, 1997].

[56] The vertical profiles in the Southern Ocean (Figures 10d–10f) present a relatively uniform distribution (down to 2 Z_{eu}) for the nanoplankton assemblages, and again show that this population is preponderant. A microplankton deep maximum seems to develop in low [Chl$a$]$_{surf}$ waters (M1 class) at about 0.8 Z_{eu}, as already documented by *Holm-Hansen and Hewes* [2004]; the statistical analysis shows a high variability of this maximum around its mean value (0.8 $\overline{\text{Chl}a}_{Zeu} \pm 0.4$).

[57] Apart from a few exceptions, the vertical distributions in mixed waters of the micro-, nano-, and pico-[Chl$a$] are practically featureless, at least within the considered layer. It is reasonable, therefore, to assume uniform profiles and simply use the results presented in Figure 9 (tabulated

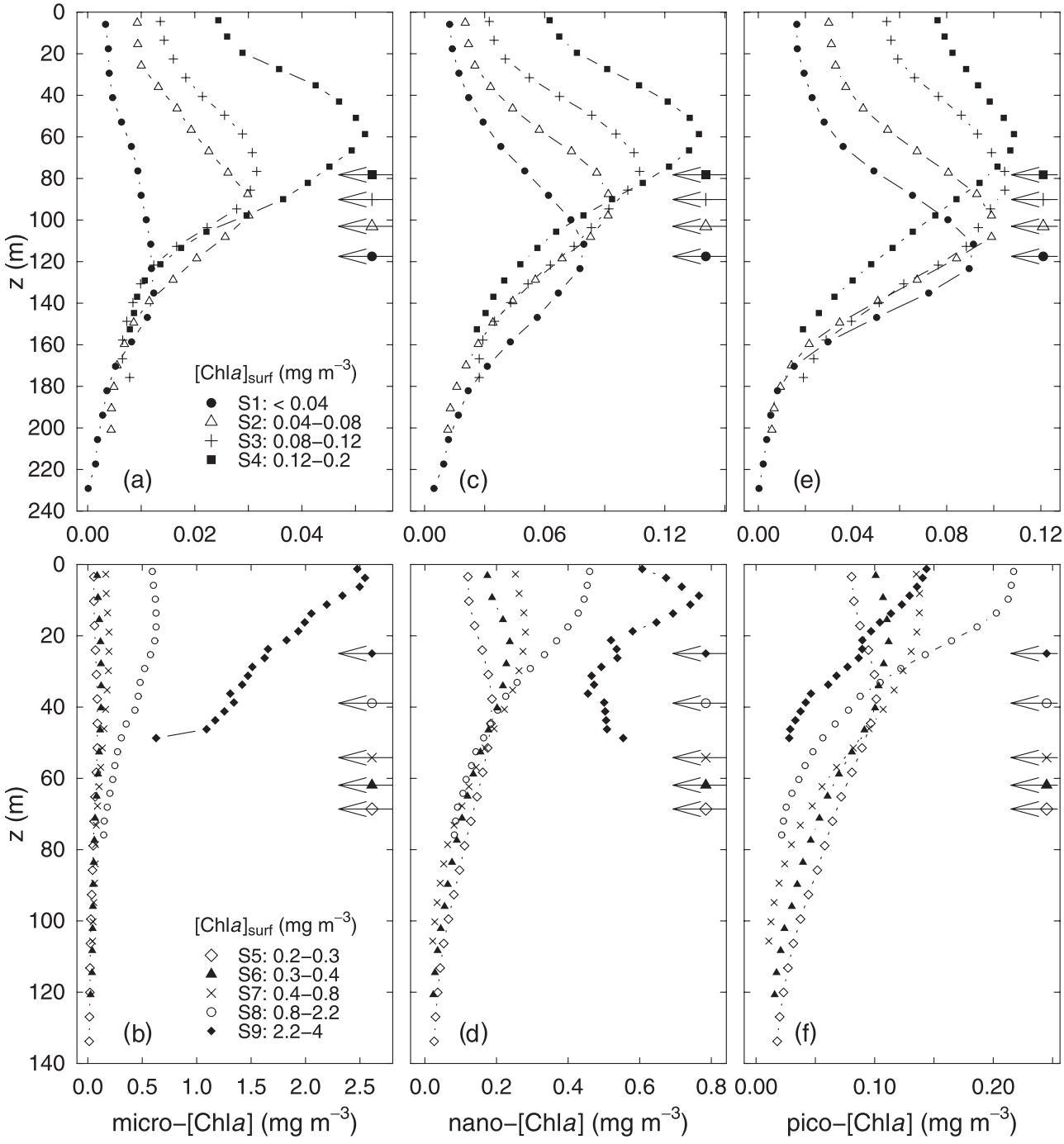

Figure 8. Same profiles as in Figure 7 after rescaling for (a and b) micro-Chl*a*, (c and d) nano-Chl*a* and (e and f) pico-Chl*a* in stratified waters. The position of Z_{eu} is indicated by an arrow identified by the symbol corresponding to its trophic category.

in Table 6), which provide the relative proportions of the micro-, nano-, and pico-[Chl*a*] as a function of [Chl*a*]$_{surf}$. Linear interpolation between the categories by using the actual [Chl*a*]$_{surf}$ value is sufficient.

5. Validating the Predicted Chlorophyll *a* Related to the Three Classes of Phytoplankton

5.1. Vertical Profiles

[58] The 20% fraction of database 1 (483 micro-, nano- and pico-[Chl*a*] vertical profiles), which was kept aside, is presently used for the validation process. These profiles were submitted to the quality control already described (see 2.1), so that those with less than 4 samples (within the euphotic zone) are discarded. It cannot be ascertained, however, that the retained profiles are able to accurately describe the actual profiles, because of the discrete nature of the samples, and often, of the adoption of fixed sampling depths. In particular, with such a protocol, a deep pigment maximum can easily be missed, even if the vertically integrated content likely is less in error. The validation

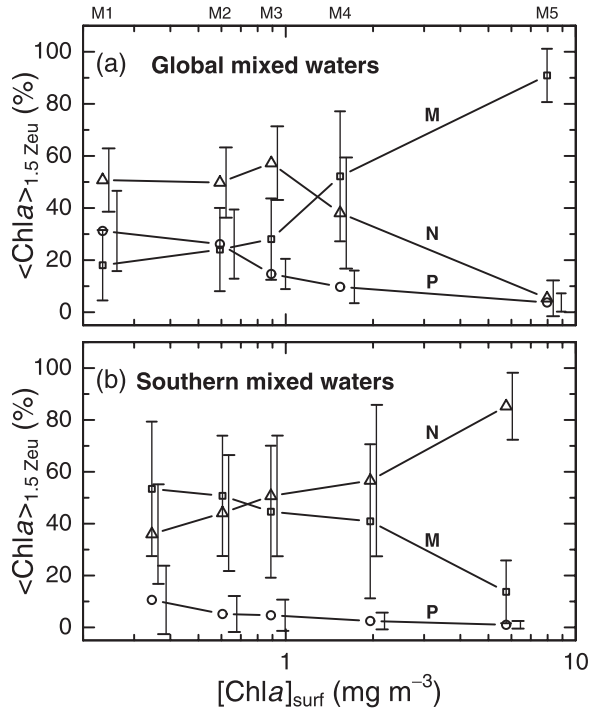

Figure 9. Composition of the phytoplankton community as a function of $[\mathrm{Chl}a]_{surf}$ for mixed waters. The average proportions (%) of micro-Chl*a*, nano-Chl*a* and pico-Chl*a*, within the 0–1.5 Z_{eu} layer, for (a) global mixed waters, southern waters excluded, and (b) Antarctic mixed waters only. The vertical bars represent ±1 SD around the mean values. The labels M, N, and P refer to microplankton, nanoplankton and picoplankton, respectively. (In the southern well-mixed waters, these labels may not be appropriate; see reservations in the text.)

exercise, however, must cope with these drawbacks, inherent to field data.

[59] The euphotic depth is computed from the $[\mathrm{Chl}a]_{surf}$ value as above, and compared to Z_m, to determine if the water column is stratified or mixed. For stratified waters, the $[\mathrm{Chl}a]_{surf}$ value is injected into the relevant parameterization to generate the three dimensionless vertical profiles; they are then rescaled in physical units by using the actual Z_{eu} and $\overline{\mathrm{Chl}a}_{Zeu}$ values. For mixed waters, uniform vertical profiles are simply derived by extrapolating downward the product of $[\mathrm{Chl}a]_{surf}$ and the relative proportion of each group.

[60] By integrating these predicted profiles from 0 to Z_{eu}, the column chlorophyll *a* contents can be computed for the three classes of phytoplankton. The predicted contents are compared to the contents obtained by integrating over the same column the actual discrete values (trapezoidal method). The stratified and mixed waters are pooled together for this comparison. Histograms of the log-transformed ratio of the predicted (vertically integrated) content to the values derived from field data are displayed in Figures 11a–11c. For the three classes, the mean and median values are very close together and both are close to zero. This means that there is no significant bias in the predictions, only a slight overestimate (by 7–14%). The geometric standard deviations (SD = 0.32 for microplankton) indicates that 68% of the ratios are within the interval 1:2 and 2:1 with respect to mean (see also the scatterplots in Figures S10 and S11 in auxiliary material); the interval is narrower for the other classes (SD = 0.21 and 0.27). In total, and for the three classes, this analysis confirms the predictive skill of the proposed parameterization when dealing with the integrated contents, and statistically quantifies its limitations.

[61] Now, and only for the stratified waters, another test can be attempted regarding the magnitude and the position of the deep maximum. The maximum chlorophyll concentrations, as predicted for the three classes, and those observed are compared in the same way as above (Figures 11d–11f). There are no notable biases (predictions underestimate the actual values by 11, 16, and 12% for the microplankton nanoplankton and picoplankton classes, respectively). The standard deviations are larger than in Figures 11a–11c. In particular, for the microplankton, the actual-to-predicted $[\mathrm{Chl}]_{max}$ ratios are within the factors 1:4 and 4:1 (for 68% of the items). The standard deviations are lesser for the two other phytoplanktonic classes. Regarding the depth of appearance of a chlorophyll maximum (Figure 11g), there is no bias, but a rather poor accuracy in the prediction of the geometrical depths. The results of these tests are satisfactory especially when considering the anticipated limitations which result from the sampling strategy.

5.2. Surface Layer

[62] This validation makes use of all the 4238 surface samples in database 2. The pigment composition for each of these samples is used to compute the fractional chlorophyll *a* concentration of the three phytoplankton groups by using equations (2a)–(2c) and (3a)–(3c). These fractional concentrations are called "measured" concentrations, in contrast to those which are predicted from the chlorophyll *a* alone.

[63] The prediction relies on the measured chlorophyll concentration, $[\mathrm{Chl}a]_{surf}$, multiplied by the respective proportions of microplankton, nanoplankton, and picoplankton, which are indexed on $[\mathrm{Chl}a]_{surf}$ (as shown in Figures 6c and 9 and Table 6). These predicted values are compared with the measured values (Figures 12a–12c, similar to Figure 11). For the three phytoplanktonic classes, there is a remarkable symmetry in the frequency distributions which are close to Gaussian ones (reduced skewness and kurtosis). There are no significant biases, except for nanoplankton (the predicted/observed ratio is around 36%). The standard deviations are rather large and decrease from the microplankton, to the nanoplankton, and to the picoplankton group, which means that the predictive skill improves. This predictive skill, however, can be judged as being generally poor (particularly for the diatoms-dinoflagellates group). Actually it reflects the natural variability within the relationships between total chlorophyll and group-specific chlorophyll. In other words, when dealing with the retrieval based on the 20% subset, the frequency distribution is identical to that one already present in the 80% subset which led to the parameterization (see Figure 6c).

[64] In preamble to the application proposed below (which deals with satellite imagery), it is worth noting that the variability observed within the group-specific and total chlorophyll relationships is similar to, albeit slightly larger than, the variability existing between total chlorophyll and chlorophyll-related bio-optical properties. For instance, the

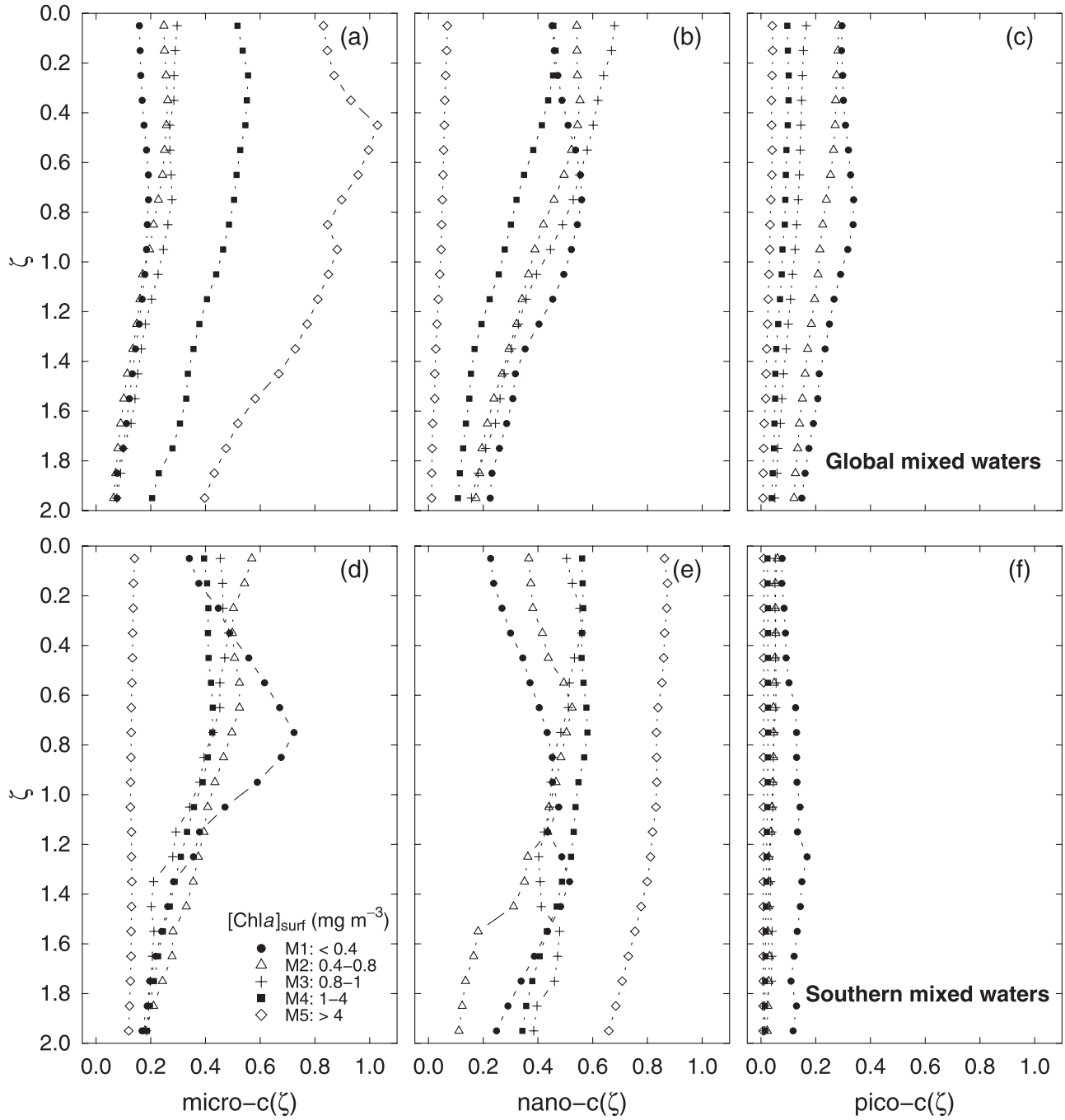

Figure 10. Average dimensionless vertical profiles of micro-Chl*a*, nano-Chl*a*, and pico-Chl*a* in mixed waters: (a–c) global mixed waters (excluding southern waters) and (d–f) southern mixed waters.

chlorophyll concentration retrieved through the recent algorithms in use for the ocean color interpretation and the in situ chlorophyll are coincident (no bias), with a geometric standard deviation (for the decimal logarithm of the ratios) which amounts to 0.22 [*O'Reilly et al.*, 2000].

6. Discussion and Conclusions

6.1. Example of Application at Global Scale of the Present Study

[65] The usefulness of the tool developed and validated here can be exemplified by applying the proposed parameterization to a global SeaWiFS image, with the objective of mapping at the world ocean scale the distribution of the three size classes, actually the three kinds of phytoplankton assemblages (see the reservation made in 2.2 about the possible lack of correlation between size classes and taxon-specific pigments). A monthly composite of the chlorophyll concentration for June 2000 is taken as an example for this application. In the same way as for primary production estimates from ocean color [e.g., *Longhurst et al.*, 1995; *Antoine et al.*, 1996; *Behrenfeld and Falkowsi*, 1997], it is assumed that the retrieval of the concentration in the near-surface layer is unbiased, so that the SeaWiFS concentration

Table 6. Average Proportions of Micro-Chl*a*, Nano-Chl*a*, and Pico-Chl*a* Within the 0–1.5 Z_{eu} Layer, for Each Trophic Category, for Stratified (S1 to S9), and Mixed Waters (M1 to M5)[a]

Trophic Class	Average $[Chla]_{surf}$, mg m^{-3}	f_{micro}, %	f_{nano}, %	f_{pico}, %
Stratified waters				
S1	0.032	7.9	44.0	48.1
S2	0.062	13.8	41.8	44.3
S3	0.098	12.7	42.1	45.2
S4	0.158	16.7	44.5	38.8
S5	0.244	23.1	49.3	27.6
S6	0.347	27.2	48.3	24.5
S7	0.540	32.5	45.2	22.2
S8	1.235	52.4	32.8	14.8
S9	2.953	74.9	21.1	4.0
Global mixed waters (southern waters excluded)				
M1	0.234	18.0	50.7	31.2
M2	0.593	24.1	49.8	26.2
M3	0.891	28.1	57.2	14.7
M4	1.540	52.2	38.1	9.7
M5	7.964	90.9	5.3	3.7
Southern mixed waters				
M1	0.345	53.4	36.0	10.6
M2	0.605	50.7	44.1	5.2
M3	0.889	44.6	50.7	4.7
M4	1.956	40.9	56.6	2.5
M5	5.755	13.7	85.3	1.0

[a]The proportions of the three groups within the euphotic layer are given in Table S3 (see auxiliary material). Proportions are in percent.

at each pixel provides the $[Chla]_{surf}$ value needed as an input for equation (7). To select the appropriate parameters (Tables 5 and 6), the stratified and mixed situations have to be discriminated, which is made on the basis of the mixed layer depth climatology for June. By using these $[Chla]_{surf}$ values, the relative proportions (in percent) of the three classes within the 0–1.5 Z_{eu} layer can be assessed on a pixel-by-pixel basis (Figures 13a–13c), as well as the corresponding vertically integrated chlorophyll contents (Figures 13d–13f). Relative proportions and integrated contents provide differing and complementary descriptions, as briefly commented in what follows.

[66] The general geographical patterns shown in Figure 13 are consistent with the current knowledge about the ecological domains and biogeochemical provinces [see, e.g., *Longhurst*, 1995], and about the preferential distribution of species [e.g., *Malone*, 1980; *Chisholm*, 1992]. The present results, however, bring new interesting information because a quantification of both the biomass and the relative contribution of each of the three size classes can be proposed. Picoplankton form the dominant group within the subtropical gyres with a relative abundance reaching 45–55% (Figure 13c), and are present everywhere in notable proportions (except in the northernmost latitude). Nevertheless, the picoplankton chlorophyll *a* biomass remains everywhere low (Figure 13f), and actually is minimal in these zones where the contribution is nonetheless maximal (i.e., in the center of the gyres). In contrast (Figures 13a and 13d), microplankton are dominant in subarctic zone (in June) and in the major coastal upwelling zones. They are also at the origin of the highest column-integrated chlorophyll contents. This diatoms and dinoflagellates population almost disappears, in proportion (< 15%) and stock (< 4 mg m^{-2}), inside the subtropical gyres, while it is present in notable proportion (20–30%) along the equator, particularly in the Pacific Ocean where small diatoms have been observed [*Chavez et al.*, 1996]. Nanoplankton behave differently, and appear to be ubiquitous with a rather stable contribution everywhere (40–50%, Figure 13b) between 50°N and 50°S. In the subarctic region. Their relative proportion, in the subarctic region, is notably depressed, although the associated stock is maximal. Within the 50°N–50°S latitudinal belt, the nanoplankton biomass is above those of the two other phytoplankton groups. A significant enhancement of this nanoplankton biomass occurs along the equator (Pacific and Atlantic Oceans), and along the subantarctic convergence.

[67] A closure is within reach, because the sum of the three fractional biomasses (Figures 13d–13f) provides the total algal chlorophyll biomass, which itself can be directly assessed by using equation (8) on a pixel-by-pixel basis with the SeaWiFS chlorophyll. If equations (1)–(3) and (8) were purely mathematical expressions, the equality of the two biomasses would be normally achieved. These equations, however, are not rigorous, and instead are best fits. They originate from independent regression analyses, one involving only chlorophyll when using equation (8) (with the A and B parameters given in Table 4 for the 0–1.5 Z_{eu} layer), whereas the others involve the full suite of pigments (equations (1)–(3)). An attempt toward a closure, therefore, comes down to a validation of the internal consistency of the two statistical approaches, which actually rests on the validity of equation (1) and the multiple regression analysis from which this equation originates.

[68] The result is especially comforting, because the global chlorophyll biomass values estimated by the two possible approaches coincide almost exactly. The fractional chlorophyll biomasses are 1.70, 3.17, and 2.55×10^{12} g Chl*a*, for the so-called microplankton, nanoplankton, and picoplankton populations, respectively. Their sum amounts to 7.43×10^{12} g Chl*a*, whereas the direct computation provides the value 7.51×10^{12} g Chl*a*. At the pixel level, deviations between the two computations are rather randomly distributed, and generally less than 1%. This global chlorophyll estimate for June is fully compatible with the yearly average (9.8×10^{12} g Chl*a*) recently proposed for the whole ocean by *Antoine et al.* [2005]. Indeed, only 77% of the ocean is represented in the SeaWiFS composite for June, because of the exclusion of residual clouds, some adjacent seas and coastal zones, and also exclusion of a major part of the Antarctic Ocean, which is unlit at this time period.

6.2. General Considerations

[69] Although the MB89 study was based on a substantial amount of data (3806 profiles), leading to rather robust results, testing this robustness was nonetheless required, in as much as an extension of the same approach was envisaged for groups of pigments, instead of chlorophyll *a* alone.

[70] The results of this preliminary test are quite satisfactory. The relationships between $[Chla]_{surf}$ and the total chlorophyll *a* column-integrated content, in both stratified and mixed waters, obtained in this study practically coincide with those obtained in MB89. This striking agreement calls for two comments: (1) the methodological change when

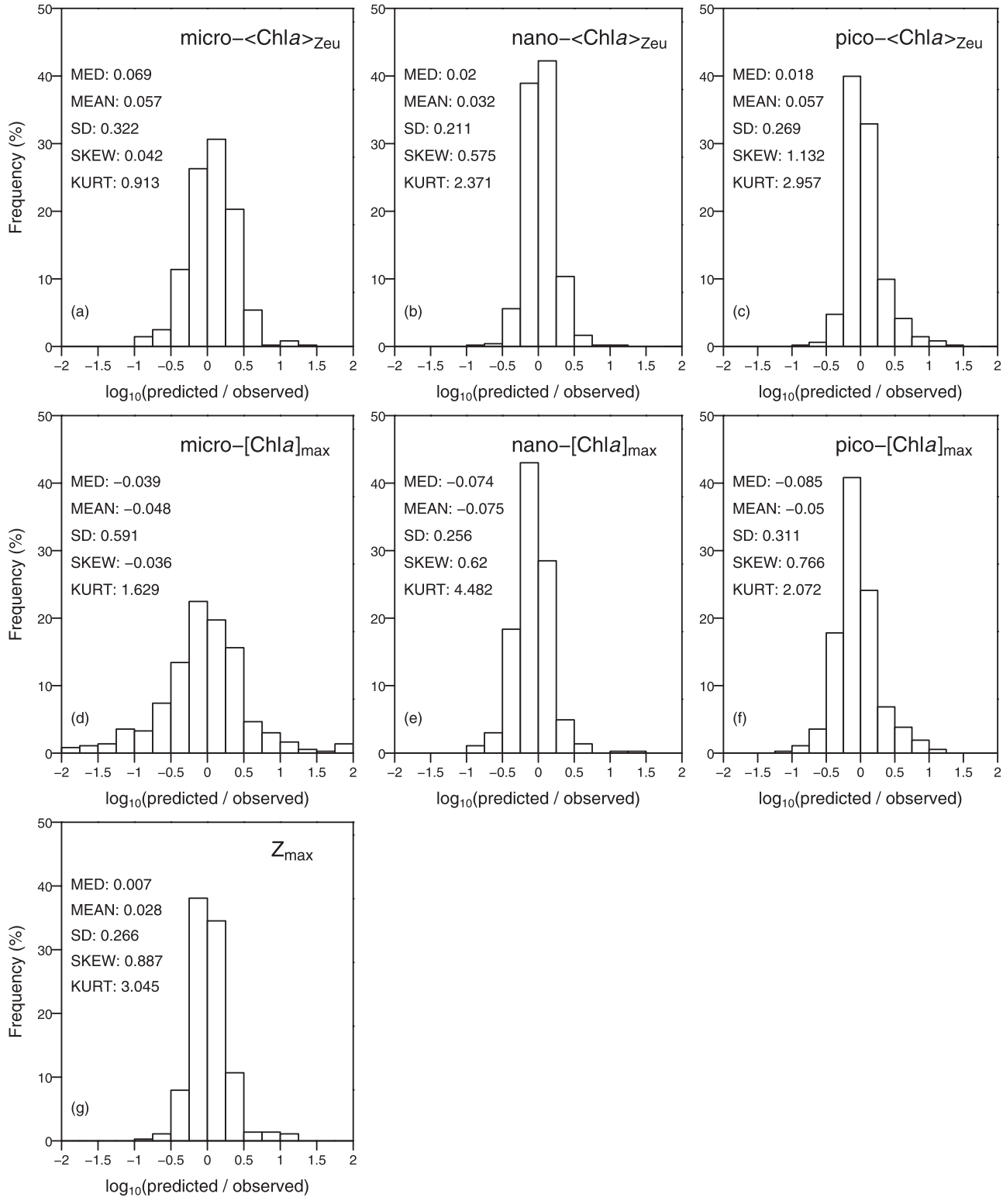

Figure 11. Frequency distribution (%) of the log-transformed ratio of the predicted/observed vertically integrated content (a–c) for stratified and mixed waters all together, (d–f) of the maximal concentration for stratified waters, and (g) of the depth of the maximal concentration for stratified waters. The frequency distribution departs from (Gaussian) normality, not because of an excessive skewness, but because of a strong leptokurtosis which concentrates the ratios around their mean.

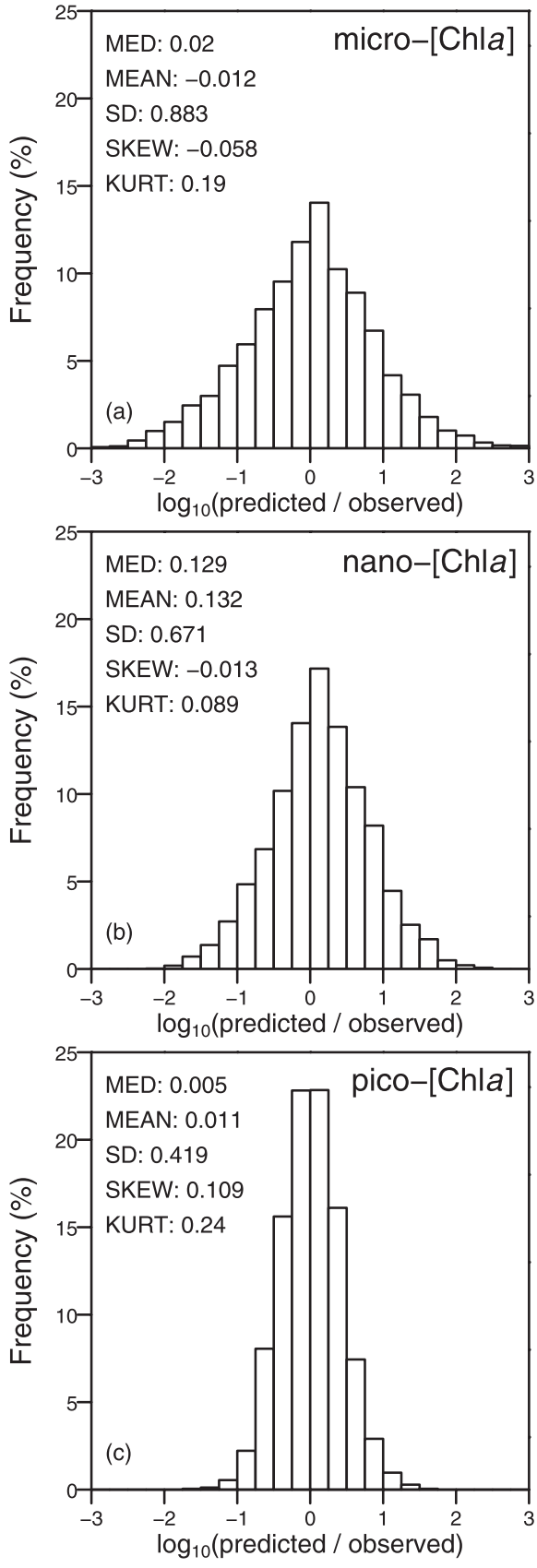

Figure 12. Frequency distribution (%) of the log-transformed ratio of the predicted/observed concentration of (a) micro-Chl*a*, (b) nano-Chl*a*, and (c) pico-Chl*a*, within surface waters only.

determining [Chl*a*] has no discernible impact upon the results, which is an indirect (and a posteriori) consolidation of the previous measurements, which were mainly based on the fluorometric method, and (2) such global relationships testify to the existence of global trends over a wide range of trophic conditions. The scatter of the data points (within a factor of about 2, as shown in Figures 3a and 3b), however, simultaneously demonstrates that these relationships are not tightly defined when a restricted range of [Chl*a*] is considered (e.g., the discussion by *Siegel et al.* [2001]).

[71] Regarding the regular and progressive change in the shapes of the vertical chlorophyll profiles along with the near-surface chlorophyll concentration, there is a close numerical agreement between the previous results and those presently obtained. This confirmation reinforces the evidence of a continuity in the linkage between vertical structure and trophic levels (both essentially ruled by physical processes). Such a continuity can be clearly discerned when the statistical analysis is performed by using dimensionless quantities, for both the depth and the concentration, whereas it remains obscure when the physical quantities are directly considered. For modeling purposes, including those for primary production based on satellite surface chlorophyll data, such a continuity is helpful and numerically easy to handle. Debates have sometimes surfaced about the comparative efficiencies of the approach based on this continuity, and of the other one involving spatial discontinuities. These discontinuities result from a partitioning of the ocean into biogeochemical provinces, each of them exhibiting for each of the four seasons fixed vertical shapes in terms of geometric depth [*Platt et al.*, 1991; *Sathyendranath et al.*, 1995]. Actually, inside a given province, and during the course of the seasons, progressive changes can take place and even smooth the boundaries with adjacent provinces. Finally the difference between the two approaches lies in the use of continuous functions or their replacement by step functions. The realization of the continuity is also supported by the regularity in the changes observed within the pigment composition and algal populations. These changes in phytoplanktonic assemblages, and the predominance of algal groups as a function of the trophic status, confirm existing general descriptions and local observations.

[72] Owing to the statistical analysis, the present study extends the previous qualitative knowledge and proposes a quantitative tool to assess the contributions of three phytoplankton groups to the total algal biomass, on the basis of a single information, which can be derived from ocean color observation. Like all statistical products, the proposed statistical relationship may fail on a case-by-case basis.

[73] Finally, this study constitutes an essential step in the synthesis of HPLC data collected during the last decade, in the context of the JGOFS program particularly. This data set provides an invaluable source allowing the distribution of the phytoplankton communities to be comprehensively described at global scales. Such a quantitative description is needed to appraise how the algal biomass interacts with carbon fluxes.

[74] The transformation of fields of biomass per size classes into fields of primary production attributable to each size class, through the use of appropriate bio-optical models, appears now feasible, to the extent that the photosyn-

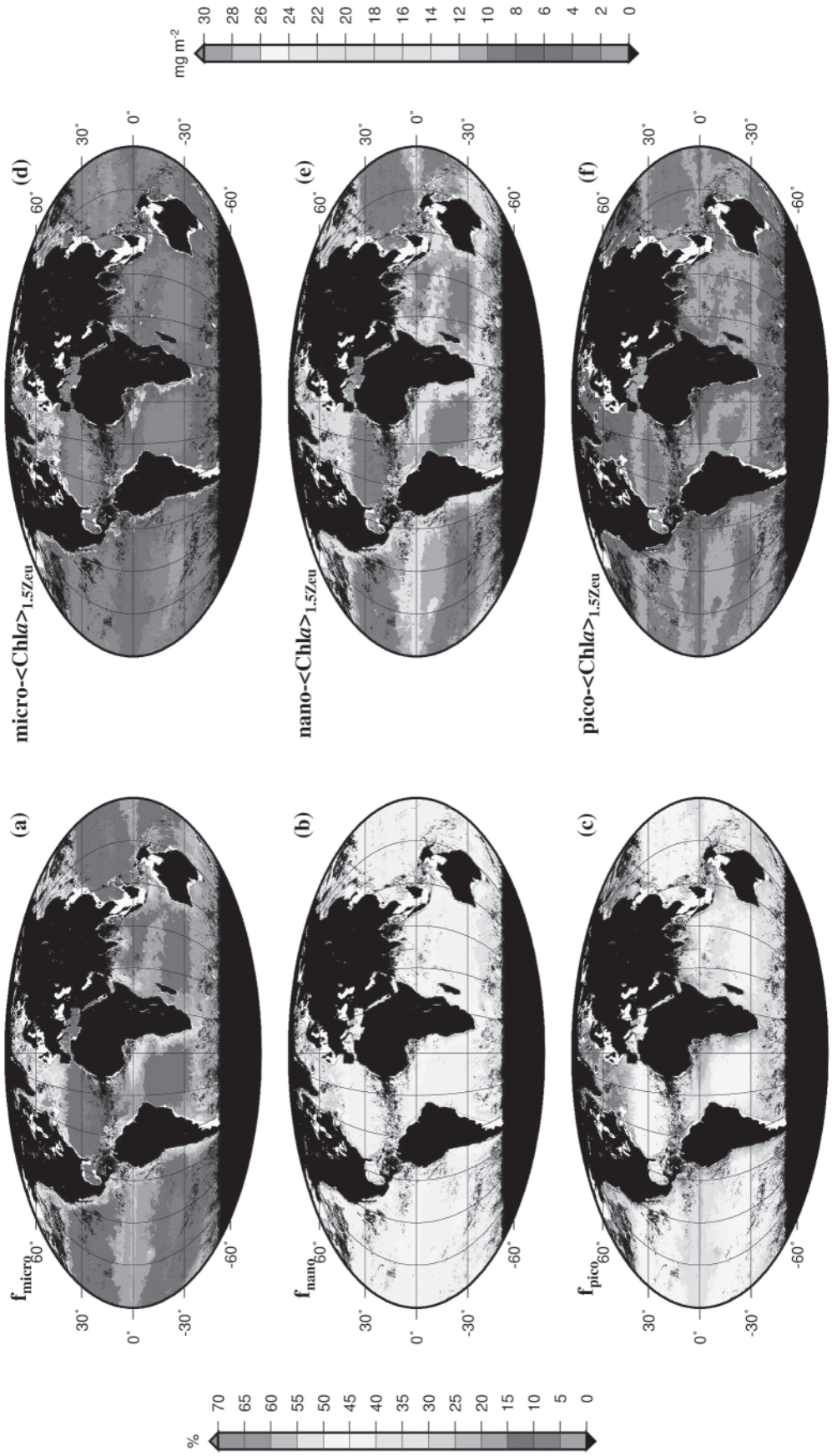

Figure 13. Phytoplankton community composition for June 2000 (SeaWiFS composite): (a–c) fractions (%) of micro-Chl*a*, nano-Chl*a* and pico-Chl*a* within the 0–1.5 Z_{eu} layer, and (d–f) integrated contents within the same layer (mg m^{-2}). Coastal areas (less than 200 m deep), large lakes and inland seas are represented in white. Red indicates a percentage of 70 and more (Figures 13a–13c), or an integrated content of 30 mg m^{-2} and more (Figures 13d–13f). Color appears in back of the print issue.

thetic parameters typical of the different phytoplankton size classes can be selected. Such fields of differentiated primary production could in turn be relevant in improving the parameterization and the validation of recent biogeochemical models which consider different phytoplanktonic compartments [e.g., *Moore et al.*, 2002; *Aumont et al.*, 2003; *Le Quéré et al.*, 2005]).

[75] **Acknowledgments.** People who kindly contributed to the implementation of the database are gratefully acknowledged: J. Aiken, K. Arrigo, R. Barlow, R. Bidigare, C. Cailliau, Y. Dandonneau, G. R. DiTullio, L. Dransfield, E. Head, H. Higgins, G. Kraay, J. C. Marty, C. Omachi, K. Oubelkheir, J. Ras, S. Roy, V. Stuart, C. Targa, D. Thibault, C. Trees, L. Van Heukelem, M. Veldhuis, F. Vidussi, G. Westbrook, S. Wright, and M. Zapata. We are also indebted to J. Ras for her participation in the early stages of the pigment database merging process. We also thank D. Antoine for helpful advice when producing the ocean color maps, B. Gentili for efficient help in computation aspects, and F. d'Ortenzio for help in using mixed layer depths climatologies. We are grateful for very constructive comments from two anonymous reviewers, which, we think, have substantially contributed to an improvement of the first version of the paper. SeaWiFS imagery was provided by the SeaWiFS project (NASA/Goddard Space Flight Center) which is duly acknowledged.

References

Antoine, D., J. M. André, and A. Morel (1996), Oceanic primary production: 2. Estimation at global scale from satellite (coastal zone color scanner) chlorophyll, *Global Biogeochem. Cycles*, *10*(1), 57–69.

Antoine, D., A. Morel, H. R. Gordon, V. F. Banzon, and R. Evans (2005), Bridging ocean color observations of the 1980s and 2000s in search of long-term trends, *J. Geophys. Res.*, *110*, C06009, doi:10.1029/2004JC002620.

Arrigo, K. R., D. L. Worthen, and D. H. Robinson (2003), A coupled ocean-ecosystem model of the Ross Sea: 2. Iron regulation of phytoplankton taxonomic variability and primary production, *J. Geophys. Res.*, *108*(C7), 3231, doi:10.1029/2001JC000856.

Aumont, O., E. Maier-Reimer, S. Blain, and P. Monfray (2003), An ecosystem model of the global ocean including Fe, Si, P colimitations, *Global Biogeochem. Cycles*, *17*(2), 1060, doi:10.1029/2001GB001745.

Behrenfeld, M. J., and P. G. Falkowski (1997), Photosynthetic rates derived from satellite-based chlorophyll concentration, *Limnol. Oceanogr.*, *42*(1), 1–20.

Boyd, P. W. (2002), Environmental factors controlling phytoplankton processes in the Southern Ocean, *J. Phycol.*, *38*, 844–861.

Campbell, J., et al. (2002), Comparison of algorithms for estimating ocean primary production from surface chlorophyll, temperature, and irradiance, *Global Biogeochem. Cycles*, *16*(3), 1035, doi:10.1029/2001GB001444.

Chavez, F. P., K. R. Buck, S. K. Service, J. Newton, and R. T. Barber (1996), Phytoplankton variability in the central and eastern tropical Pacific, *Deep Sea Res., Part II*, *43*(4–6), 835–870.

Chisholm, S. W. (1992), Phytoplankton size, in *Primary Productivity and Biogeochemical Cycles in the Sea*, edited by P. G. Falkowski and A. D. Woodhead, pp. 213–237, Springer, New York.

Claustre, H. (1994), The trophic status of various oceanic provinces as revealed by phytoplankton pigment signatures, *Limnol. Oceanogr.*, *39*(5), 1206–1210.

Claustre, H., M. A. Moline, and B. B. Prezelin (1997), Sources of variability in the column photosynthetic cross section for Antarctic coastal waters, *J. Geophys. Res.*, *102*(C11), 25,047–25,060.

Claustre, H., et al. (2004), An intercomparison of HPLC phytoplankton methods using in situ samples: Application to remote sensing and database activities, *Mar. Chem.*, *85*(1–2), 41–61.

Cota, G. F., W. G. Harrison, T. Platt, S. Sathyendranath, and V. Stuart (2003), Bio-optical properties of the Labrador Sea, *J. Geophys. Res.*, *108*(C7), 3228, doi:10.1029/2000JC000597.

de Boyer Montégut, C., G. Madec, A. S. Fischer, A. Lazar, and D. Iudicone (2004), Mixed layer depth over the global ocean: An examination of profile data and a pofile-based climatology, *J. Geophys. Res.*, *109*, C12003, doi:10.1029/2004JC002378.

Eppley, R. W., and B. J. Peterson (1979), Particulate organic matter flux and planktonic new production in the deep ocean, *Nature*, *282*, 677–680.

Gibbs, R. J. (1979), Chlorophyll *b* interference in the fluorometric determination of chlorophyll *a* and phaeo-pigments, *Aust. J. Mar. Freshwater Res.*, *30*, 597–606.

Gieskes, W. W. C., G. W. Kraay, A. Nontji, D. Setiapermana, and Sutomo (1988), Monsoonal alternation of a mixed and a layered structure in the phytoplankton of the euphotic zone of the Banda Sea (Indonesia): A mathematical analysis of algal pigment fingerprints, *Neth. J. Sea Res.*, *22*(2), 123–137.

Goffart, A., G. Catalano, and J. H. Hecq (2000), Factors controlling the distribution of diatoms and Phaeocystis in the Ross Sea, *J. Mar. Syst.*, *27*(1–3), 161–175.

Goldman, J. C. (1993), Potential role of large oceanic diatoms in new primary production, *Deep Sea Res.*, *40*, 159–168.

Gordon, H. R., and W. R. McCluney (1975), Estimation of the Depth of sunlight penetration in the sea for remote sensing, *Appl. Opt.*, *14*(2), 413–416.

Gordon, H. R., and A. Morel (1983), *Remote Assessment of Ocean Color for Interpretation of Satellite Visible Imagery: A Review*, 114 pp., Springer, New York.

Holm-Hansen, O., and C. D. Hewes (2004), Deep chlorophyll-a maxima (DCMs) in Antarctic waters, *Polar Biol.*, *27*(11), 699–710.

Jeffrey, S. W., and M. Vesk (1997), Introduction to marine phytoplankton and their pigment signatures, in *Phytoplankton Pigment in Oceanography: Guidelines to Modern Methods*, edited by S. W. Jeffrey, R. F. C. Mantoura, and S. W. Wright, pp. 33–84, UNESCO, Paris.

Le Quéré, C., et al. (2005), Ecosystem dynamics based on plankton functional types for global ocean biogeochemistry models, *Global Change Biol.*, *11*, 2016–2040.

Letelier, R. M., D. M. Karl, M. R. Abbott, and R. R. Bidigare (2004), Light driven seasonal patterns of chlorophyll and nitrate in the lower euphotic zone of the North Pacific Subtropical Gyre, *Limnol. Oceanogr.*, *49*(2), 508–519.

Lewis, M. R., J. J. Cullen, and T. Platt (1983), Phytoplankton and thermal structure in the upper ocean: Consequences of nonuniformity in chlorophyll profile, *J. Geophys. Res.*, *88*, 2565–2570.

Longhurst, A. R. (1995), Seasonal cycles of pelagic production and consumption, *Prog. Oceanogr.*, *36*, 77–167.

Longhurst, A. R., S. Sathyendranath, T. Platt, and C. M. Caverhill (1995), An estimate of global primary production in the ocean from satellite radiometer data, *J. Plankton Res.*, *17*(6), 1245–1271.

Malone, T. C. (1980), Algal size, in *The Physiological Ecology of Phytoplankton*, edited by I. Morris, pp. 433–463, Univ. of Calif., Berkeley.

Mantoura, R. F. C., R. G. Barlow, and E. J. H. Head (1997), Simple isocratic HPLC methods for chlorophylls and their degradation products, in *Phytoplankton Pigment in Oceanography: Guidelines to Modern Methods*, edited by S. W. Jeffrey, R. F. C. Mantoura, and S. W. Wright, pp. 383–428, UNESCO, Paris.

Moline, M. A., and B. B. Prézelin (1996), Long-term monitoring and analyses of physical factors regulating variability in coastal Antarctic phytoplankton biomass, in situ productivity and taxonomic composition over subseasonal, seasonal and interannual time scales, *Mar. Ecol. Prog. Ser.*, *145*(1–3), 143–160.

Monterey, G., and S. Levitus (1997), *Seasonal Variability of Mixed Layer Depth for the World Ocean, NOAA Atlas NESDIS, 14*, 96 pp., U. S. Govt. Print. Off., Washington, D. C.

Moore, J. K., S. C. Doney, J. A. Kleypas, D. M. Glover, and I. Y. Fung (2002), An intermediate complexity marine ecosystem model for the global domain, *Deep Sea Res.*, *49*(1–3), 403–462.

Morel, A. (1988), Optical modeling of the upper ocean in relation to its biogenous matter content (case 1 waters), *J. Geophys. Res.*, *93*(C9), 10,749–10,768.

Morel, A., and J. F. Berthon (1989), Surface pigments, algal biomass profiles, and potential production of the euphotic layer: Relationships reinvestigated in view of remote-sensing applications, *Limnol. Oceanogr.*, *34*(8), 1545–1562.

Morel, A., and S. Maritorena (2001), Bio-optical properties of oceanic waters: A reappraisal, *J. Geophys. Res.*, *106*(C4), 7163–7180.

Ondrusek, M. E., R. R. Bidigare, S. T. Sweet, D. A. Defreitas, and J. M. Brooks (1991), Distribution of phytoplankton pigments in the North Pacific Ocean in relation to physical and optical variability, *Deep Sea Res.*, *38*(2), 243–266.

O'Reilly, J. E., S. Maritorena, D. A. Siegel, S. A. Garver, M. Kahru, and C. McClain (1998), Ocean chlorophyll algorithms for SeaWiFS, *J. Geophys. Res.*, *103*(C11), 24,937–24,953.

O'Reilly, J. E., et al. (2000), Ocean color chlorophyll a algorithms for SeaWiFS OC2 and OC4, version 4, in *SeaWiFS Postlaunched Calibration and Validation Analyses, Part 3*, edited by S. B. Hooker and E. R. Firestone, *NASA Tech. Memo. 2000-206892, 11*, 9–23, NASA.

Platt, T., C. Caverhill, and S. Sathyendranath (1991), Basin-scale estimates of oceanic primary production by remote sensing: The North Atlantic, *J. Geophys. Res.*, *96*(C8), 15,147–15,159.

Prézelin, B. B., E. E. Hofmann, C. Mengelt, and J. M. Klinck (2000), The linkage between Upper Circumpolar Deep Water (UCDW) and phytoplankton assemblages on the west Antarctic Peninsula continental shelf, *J. Mar. Res.*, *58*(2), 165–202.

R Development Core Team (2004), *R: A Language And environment for Statistical Computing*, R Found. for Stat. Comput., Vienna, Austria. (Available at http://www.R-project.org)

Sathyendranath, S., A. R. Longhurst, C. M. Caverhill, and T. Platt (1995), Regionally and seasonally differentiated primary production in the North Atlantic, *Deep Sea Res., Part I*, *42*(10), 1773–1802.

Sathyendranath, S., G. Cota, V. Stuart, H. Maass, and T. Platt (2001), Remote sensing of phytoplankton pigments: A comparison of empirical and theoretical approaches, *Int. J. Remote Sens.*, *22*(2–3), 249–273.

Siegel, D. A., et al. (2001), Bio-optical modeling of primary production on regional scales: The Bermuda BioOptics project, *Deep Sea Res.*, *48*(8–9), 1865–1896.

Stramska, M., D. Stramski, R. Hapter, S. Kaczmarek, and J. Ston (2003), Bio-optical relationships and ocean color algorithms for the north polar region of the Atlantic, *J. Geophys. Res.*, *108*(C5), 3143, doi:10.1029/2001JC001195.

Trees, C. C., D. K. Clark, R. R. Bidigare, M. E. Ondrusek, and J. L. Mueller (2000), Accessory pigments versus chlorophyll *a* concentrations within the euphotic zone: A ubiquitous relationship, *Limnol. Oceanogr.*, *45*(5), 1130–1143.

Vidussi, F., H. Claustre, B. B. Manca, A. Luchetta, and J. C. Marty (2001), Phytoplankton pigment distribution in relation to upper thermocline circulation in the eastern Mediterranean Sea during winter, *J. Geophys. Res.*, *106*(C9), 19,939–19,956.

H. Claustre, A. Morel, and J. Uitz, Laboratoire d'Océanographie de Villefranche, CNRS UMR 7093, and Université Pierre et Marie Curie, B.P. 08, F-06238 Villefranche-sur-Mer cedex, France. (uitz@obs-vlfr.fr)

S. B. Hooker, Laboratory for Hydrospheric Processes, NASA/Goddard Space Flight Center, Greenbelt, MD 20771, USA.

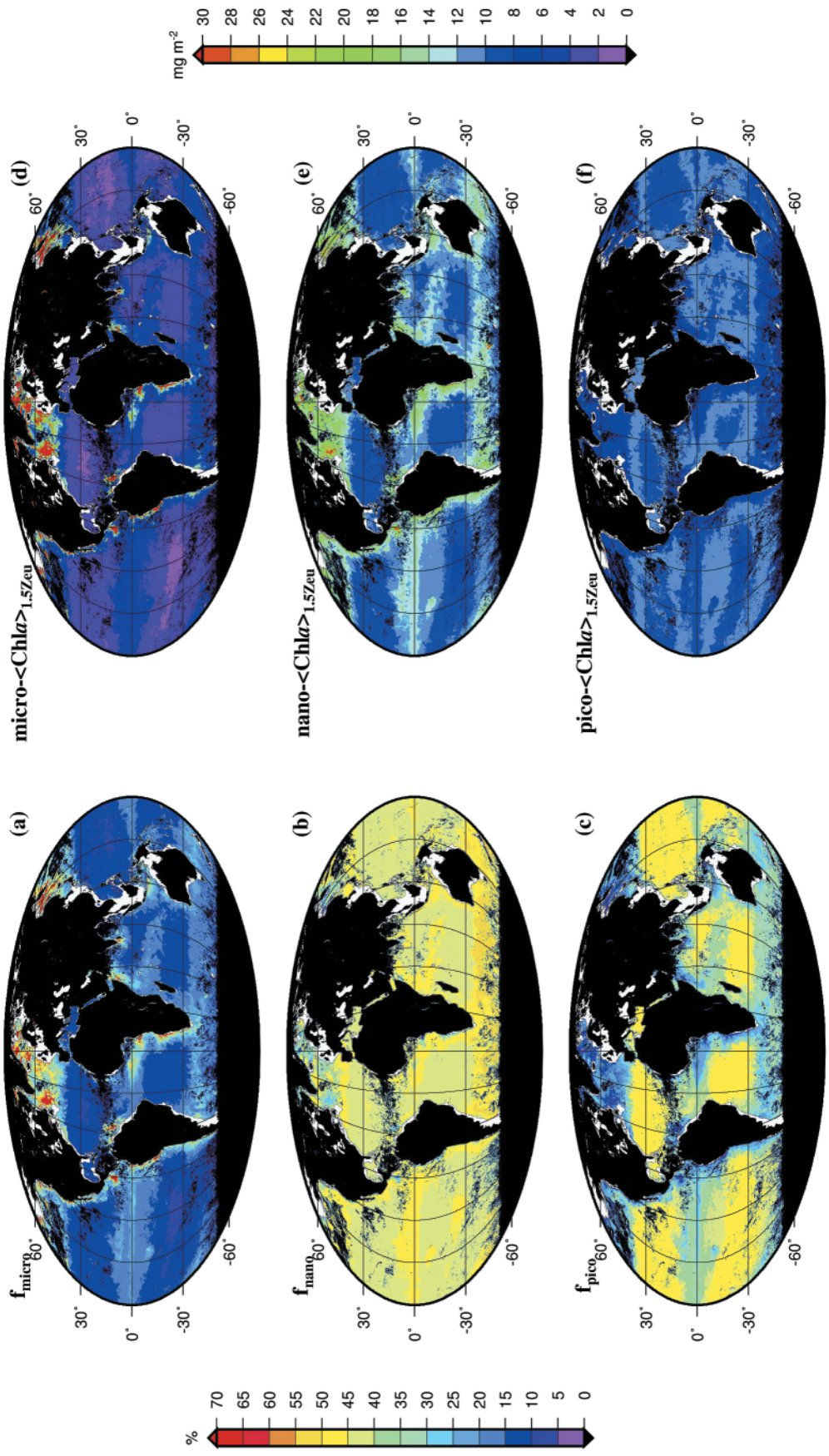

Figure 13. Phytoplankton community composition for June 2000 (SeaWiFS composite): (a–c) fractions (%) of micro-Chl*a*, nano-Chl*a* and pico-Chl*a* within the 0–1.5 Z_{eu} layer, and (d–f) integrated contents within the same layer (mg m^{-2}). Coastal areas (less than 200 m deep), large lakes and inland seas are represented in white. Red indicates a percentage of 70 and more (Figures 13a–13c), or an integrated content of 30 mg m^{-2} and more (Figures 13d–13f).